Research Square

Preprints are preliminary reports that have not undergone peer review.
They should not be considered conclusive, used to inform clinical practice,
or referenced by the media as validated information.

# Isolation, Characterization, and Biomedical Potential of Phycoerythrin Phycobiliprotein from Kappaphycus alvarezii (Doty) Doty ex Silva: Antimicrobial, Antioxidant, and Anticancer Activities

**Harinathan Balasundaram**
Krishna Institute of Allied Sciences
**Parthasarathy Seethapathy**
Amrita School of Agricultural Sciences, Amrita Vishwa Vidyapeetham
**Subbiah Sankaralingam**
Virudhunagar Hindu Nadars and Senthikumara Nadar College
**Shunmugiah Mahendran**
Ayya Nadar Janaki Ammal College (Autonomous)
**Murugan Mareeswaran**
Ayya Nadar Janaki Ammal College (Autonomous)
**Jeyaraj Pandiarajan**
Ayya Nadar Janaki Ammal College (Autonomous)
**Pandiaraj Maheswari**
Ayya Nadar Janaki Ammal College (Autonomous)
**Sakthivel Venkatesh**
Virudhunagar Hindu Nadars and Senthikumara Nadar College
**Malaisamy Arunkumar**
International Centre for Genetic Engineering and Biotechnology (ICGEB)
**Girish R. Pathade**
Krishna Institute of Allied Sciences
**Deepu Pandita**
deepupandita@gmail.com

Government Department of School Education, Jammu, Jammu and Kashmir 180001, India
**Anu Pandita**
Vatsalya Clinic
**Fazal Ullah**
Northwest Normal University
**Hosam O. Elansary**
King Saud University

**Muhammad Nazim**
Chinese Academy of Sciences
**Adel A. Fickak**
King Saud University
**Mohamed A. Rashwan**
King Saud University
**Ihab Mohamed Moussa**
King Saud University

---

**Article**

**Keywords:** Bioactive molecules, Lung cancer, Molecular docking, Phycoerythrin, Pigment analysis, Red seaweed

**Posted Date:** January 30th, 2025

**DOI:** https://doi.org/10.21203/rs.3.rs-5880917/v1

**License:** This work is licensed under a Creative Commons Attribution 4.0 International License. Read Full License

**Additional Declarations:** No competing interests reported.

---

**Version of Record:** A version of this preprint was published at Scientific Reports on July 31st, 2025. See the published version at https://doi.org/10.1038/s41598-025-11899-7.

# Abstract

*Kappaphycus alvarezii* (Doty) Doty ex Silva, a red seaweed widely cultivated for carrageenan polysaccharide, is also a potential source of the valuable pigment phycoerythrin (PE). Therefore, this study aims to extract phycoerythrin from *K. alvarezii*, evaluate its antimicrobial, antioxidant, and anticancer activities, and identify its biomedical potential for future therapeutic applications. The protein content of phycoerythrin pigment extracted from *K. alvarezii* was found to be 69.84% and showed excellent antimicrobial activity against *Klebsiella oxytoca* and *Proteus mirabilis*, with a minimum inhibition zone of 11 mm. It showed significant *in vitro* antioxidant activity, as analyzed using total antioxidant, hydrogen peroxide scavenging, reducing power, DPPH, and ABTS assays. Further, the pigment exhibited potent cytotoxicity against a human lung cancer cell line, with an $IC_{50}$ value of 131.7 μg $mL^{-1}$. Furthermore, increasing the concentration of phycoerythrin pigment decreased the cell proliferation and induced apoptosis, as confirmed by Annexin V/PI staining. Comprehensive characterization using FT-IR, HPLC, and GC-MS analysis revealed the nature of pigment and functional groups, highlighting its potential for biomedical applications. The molecular docking of *K. alvarezii*-derived compounds revealed significant binding affinities with 13 antibacterial target proteins. These results highlight the potential of *K. alvarezii* bioactive compounds as promising antibacterial agents. The phycoerythrin extract from *K. alvarezii* demonstrated potent antimicrobial, antioxidant, and anticancer properties, with significant cytotoxicity against lung cancer cells and confirmed apoptosis induction. Structural analysis revealed its bioactive composition, emphasizing its potential as a natural therapeutic agent. These findings support its potential application in biomedical and pharmaceutical industry.


# Introduction

Marine organisms produce a diversified array of bioactive compounds including carbohydrates, lipids, proteins, polyphenols, minerals, amines, amides, antioxidants, and pigments with unique molecular structures and varied biological functions [1]. Currently, these bioactive compounds are recognized as valuable sources for the food and health care sectors [2]. Therefore, there has been a rising attention in the research and development focusing on commercial exploitation of marine organisms derived bioactive primary and secondary metabolites as an ecofriendly and effective alternate for synthetic drugs [3]. In recent years, the discovery of unique bioactive substances with significant dietary, nutraceutical and medicinal advantages has attracted significant attention to marine algae.

Marine algae are essential components of the food chain, constituting over 70% of the global living biomass [2]. Marine algae are photosynthetic organisms both macroscopic and microscopic, that have garnered attention due to their immense potential as a sustainable and environmentally friendly source for several bioactive compounds [4]. Marine algae or seaweed are growing habitually through autotrophic, mixotrophic, or heterotrophic ways [5]. The potential of marine algae to be cultivated in fresh, saline and waste waters, along with their fast multiplication, presents them as an attractive substitute for diverse products, thereby conserving time and resources [6]. Seaweeds are divided into three categories based on their photosynthetic pigments: green macroalgae, brown macroalgae, and red

macroalgae. Among these, red macroalgae account for over 60% of the 30,000 tons of algae produced globally [7]. A variety of red macroalgae are rich in bioactive compounds, making them a preferred choice for the production of commercially valuable bioproducts such as biofertilizers, biofuels, colorants, cosmetics, food, hydrocolloids, nutraceuticals, pharmaceuticals, plant stimulants and thickeners [8].

*Kappaphycus alvarezii* (Doty) Doty ex. Silva (elkhorn sea moss) of family Solieriaceae, is a red seaweed (macroalgae) and is the primary carrageenophyte, commercially known as “cottoni”. It is mostly cultivated to produce commercial *kappa*-carrageenan hydrocolloids in both habitual and non-indigenous areas and has gained potential economic value in the seaweed industry. This macroalgae is the fifth most cultivated in the world, especially in various tropical countries of Asia and Africa, including India [7], due to its fast growing rates, simple cultivation process, high biomass yield in a short time with high polysaccharide content, and low investment requirements [9]. It also serves as a food source for local populations in Southeast Asia and is believed to possess various health benefits. The yellowish, reddish, green, and brown colors of *K. alvarezii* are based on the levels of phycoerythrin protein pigment [10]. The highly variable chemical components and quantities in *K. alvarezii* are influenced by the cultivation conditions, including water temperature, salinity, radiation, environmental variables, light level, profundity, and wave strength. On average, *K. alvarezii* consists of 50.8% carbohydrates, 15.6% ash, 12.4% sulphated groups, 3.3% proteins, 3.3% lipids, and 3.0% insoluble aromatics [8]. The literature indicates extensive use of *K. alvarezii* for carrageenan extraction. Furthermore, reports suggest that extracts of *K. alvarezii* possesses a multitude of essential compounds and high-value molecules with antioxidant and anti-inflammatory, antitumor, antiviral, antidiabetic, antihyperlipidemic activities, and for neural dysfunction properties [7, 11, 12].

Cancer is a fatal disease that poses a significant risk to individuals worldwide, ranking as the second most common cause of mortality in numerous countries. In 2022, the global community experienced 20 million new cases of cancer and 9.7 million fatalities associated with this disease [13]. Lung cancer ranks among the most common cancers and is a primary contributor to cancer-related fatalities worldwide [14]. Patients diagnosed with lung cancer encounter a higher risk of meeting bacterial infections, which can vary from mild cases to those that pose significant threats to life. Both bacteria and viruses have the capability to trigger inflammatory cells and activate inflammatory signaling pathways. In particular, *Escherichia coli* (Migula 1895) Castellani and Chalmers 1919, *Pseudomonas aeruginosa* (Schröter 1872) Migula 1900, *Staphylococcus aureus* Rosenbach 1884, and *Klebsiella* sp. are gram-negative bacteria that are often found in the lungs of cancer patients [15, 16]. These bacteria are often found along with other factors like age-related illnesses, large tumors, and rapid clinical decline [17]. The currently available cancer medications are come with more physical and psychological side effects like pain, vomiting, diarrhea, exhaustion, and nausea; thus, the cancer therapies cannot be considered safe [18]. Consequently, it is essential to explore novel anticancer medications sourced from nature that are safe, affordable, and less detrimental. The anti-cancer capability of *K. alvarezii* could be due to polysaccharides, nutrients, and other metabolites with antioxidant potential [19]. The phycobiliprotein (PBPs) family includes phycoerythrin (PE), which are macromolecular compounds in most macroalgal species. These proteins assemble to form a super-molecular protein complex called

phycobilisome, with linkers joining the sub-units [20]. PBPs from red macroalgae species are essential as anticancer and anti-bacterial drugs. They have the potential to enhance the efficacy of conventional anticancer medications while simultaneously mitigating their adverse effects. Additionally, they can function as photosensitizers for the treatment of infected cells [21].

Microorganisms, medicinal plants, and marine algae are the primary sources of most cancer medications. Although red seaweed proteins and pigments hold significant prospects for the advancement of nutraceuticals and pharmaceuticals for cancer treatments, substantial gaps in our understanding remain [11, 22]. Multiple factors, including their source, extraction methods, and human physiological reactions, effectiveness of algal compounds, requiring a thorough understanding to fully harness their advantages and commercial exploitation. Furthermore, the uses of these pigments and their derivatives in the context of cancer treatment remain largely unexamined. The present study aims to highlight the anticancer effects of phycoerythrin derived from *K. alvarezii* through its application in human lung cancer cell lines. This article examines the potential of phycoerythrin (PE), a red protein-pigment complex derived from *K. alvarezii*, as a promising candidate with potential for anticancer drug with a possible treatment for lung cancer. The purified phycoerythrin was tested *in vitro* for its antimicrobial, antioxidant and anticancer activities, and *K. alvarezii* derived metabolites was evaluated for the first time through virtual screening and molecular docking analyses.

## Materials and methods

# Source of seaweed

The red seaweed *K. alvarezii* was collected alive and healthy from the Mandapam coast (9.2770°N, 79.1252°E) in Rameshwaram, India, and the formal identification was confirmed. We meticulously cleaned the seaweed samples in seawater to remove any superfluous material, including epiphytes and non-living matter, before transporting them to the laboratory in plastic containers. Then, they were thoroughly cleaned and rinsed with sterile distilled water prior to the extraction process.

## Extraction of phycoerythrin

*K. alvarezii* was cut into small fragments, ground using a sterile pestle and mortar, and transferred to a 250 mL beaker. Sodium phosphate buffer (pH 7.4) was prepared using the required chemicals. The buffer was added to the ground seaweed, and the mixture was subject to a freeze-thaw cycle at -20°C and 37°C. The sample was subsequently centrifuged at 8000 rpm for 15 min. The pellet was discarded, and the supernatant was analyzed for phycoerythrin pigments utilizing a UV/ Vis spectrophotometer at wavelengths of 562, 615, and 652 nm (Beckman, USA) [23].

## Purification of phycoerythrin

The isolated phycoerythrin pigment was saturated with ammonium sulfate 60% concentration by continuous stirring at 4°C. Ammonium sulfate was slowly added until saturation was achieved. The phycoerythrin extract was stirred overnight and then centrifuged at 8000 rpm for 15 min at 4°C. The obtained pellet was collected, dried, and prepared for further analysis. To partially purify the phycoerythrin, the extract was subjected to dialysis. The pellet obtained from ammonium sulfate precipitation was placed in a dialysis bag and dialyzed against sterile distilled water until the bag shrank, and the pigment was purified. Preliminary purification was further conducted using gel permeation chromatography with a Sephadex G-100 column. To achieve this process, a 30 × 2 cm column was prepared and equilibrated with 150 mL of sodium phosphate buffer (pH 7). A 10 mL dialyzed and filtered phycoerythrin sample was loaded onto the column. A linear gradient of sodium phosphate buffer, ranging from pH 5 to 8.2, was used to elute the sample. Fractions of 5 mL were collected at a constant flow rate of 20 mL $h^{-1}$. The absorption spectrum of the purified phycoerythrin was measured using a UV/Vis spectrophotometer in the wavelength range of 300–750 nm. The total protein concentration was determined using Lowry's method.

## Characterization of phycoerythrin

# Fourier transform infrared (FT-IR) spectroscopy analysis

The Perkin-Elmer FT-IR instrument was used to examine IR spectroscopy of phycoerythrin, facilitating the analysis of various sulfate, carboxyl, and hydroxyl groups contained in the purified phycoerythrin pigment.

# High-performance liquid chromatography (HPLC) analysis

The phycoerythrin was separated using a C18 system column (LC-10VP Shimadzu) and eluted with sterile distilled water at a flow rate of 1.0 mL $min^{-1}$ at 20°C. A refractive index detector was used to keep track of the separated components. HPLC was used to examine the sugar composition of the seaweed extract after it had been hydrolyzed and treated with methanol. The column was calibrated using molecular mass standards and a standard curve was established.

## Gas chromatography–mass spectrometry (GC-MS) analysis

The GC-2010 (GCM-QP 2010) SHIMADZU gas chromatography apparatus, equipped with a flame-ionization detector (FID) and a split injector, was used to analyze phycoerythrin. High-purity helium served as the carrier gas at a flow rate of 1.40 mL $min^{-1}$. The column temperature was maintained at 200°C, while the splitter temperature was set to 240°C. A 1 µL sample of dichloromethane was injected through a glass-lined splitter with a split ratio of 1:90. Absorption was measured within the mass-to-charge (m/z) range of 40 to 800. To facilitate visualization by comparing the mass spectra of the components with those from the NIST 14 mass spectral database.

## Antibacterial activity of phycoerythrin

The antibacterial activity of phycoerythrin was evaluated using the well-diffusion method against seven clinical pathogens such as *Bacillus subtilis* (Ehrenberg 1835) Cohn 1872, *Escherichia coli*, *Klebsiella oxytoca* (Flügge 1886) Lautrop 1956, *Proteus mirabilis* Hauser 1885, *Pseudomonas aeruginosa*, *Staphylococcus aureus*, and *Streptococcus pyogenes* Rosenbach 1884. These bacterial strains were obtained from the Department of Microbiology, Ayya Nadar Janaki Ammal College, Sivakasi, India. Using a sterile cotton swab, 24-hour-old bacterial cultures were aseptically swabbed on Mueller-Hinton agar plates. Wells were loaded with phycoerythrin at a concentration of 30 µg, while Ampicillin at 50 µg served as positive control. The plates were incubated at 35°C for 24 h. After incubation, the diameter of the inhibitory zones around each well was measured (mm) and recorded.

### In vitro antioxidant activity of phycoerythrin

## Determination of total antioxidant capacity

The total antioxidant activity of phycoerythrin was assessed using the method described by [24]. A reaction mixture was prepared by combining 3.0 mL of reagent solution (containing 0.6 M sulfuric acid, 28 mM sodium phosphate, and 4 mM ammonium molybdate) with 0.3 mL of the phycoerythrin sample. The mixture was incubated in a water bath at 95°C for 90 min. After 15 min of cooling, the absorbance of all samples was measured at 695 nm, along with ascorbic acid as a control.

## Determination of reducing power

The reducing power of phycoerythrin was determined by using the method described by [25]. A 4 mL reaction mixture, consisting of phycoerythrin samples at various concentrations in phosphate buffer (0.2 M, pH 6.6), was incubated with 1% (w/v) potassium ferricyanide at 50°C for 20 min. The reaction was stopped by adding 10% (w/v) trichloroacetic acid (TCA) solution. The resulting solution was mixed with distilled water and 0.1% (w/v) ferric chloride solution. The absorbance was then measured at 700 nm using a UV/ Vis spectrophotometer.

## Hydrogen peroxide scavenging assay

The free radical scavenging activity of phycoerythrin was determined using the hydrogen peroxide assay [26]. A 10 mM hydrogen peroxide solution was prepared in phosphate-buffered saline (0.1 M, pH 7.4). To perform the assay, 1 mL of the extract at varying concentrations (100, 250, 500, 750, and 1000 µg) was mixed with 2 mL of the hydrogen peroxide solution. The mixture was incubated at 37°C for 10 min. The absorbance was measured at 230 nm using a UV/ Vis spectrophotometer, with a blank (without hydrogen peroxide) used as the reference.

## DPPH radical scavenging assay

The free radical scavenging activity of phycoerythrin was assessed using the 1,1-diphenyl-2-picryl-hydrazyl (DPPH) method using spectrophotometry [27]. DPPH, a simple and reliable reagent, was used to

evaluate the oxidizable groups in natural or synthetic antioxidants. A 0.1 mM DPPH solution in methanol was prepared, and 1 mL of this solution was added with 3 mL of varying concentrations of phycoerythrin (100, 250, 500, 750, and 1000 µg). The absorbance was measured at 517 nm after 10 min.

# ABTS inhibition assay

The ability of phycoerythrin to scavenge the 2,2'-azinobis (3-ethylbenzothiazoline-6-sulfonic acid) diammonium salt (ABTS) radical was determined using the method described in [28]. ABTS was made by combining 5 mL of 7 mM ABTS with 88 µL of 140 mM potassium persulfate, and the mixture was kept in the dark at room temperature for 16 h. The solution was then diluted with 50% ethanol until its absorbance at 734 nm reached 0.7 ± 0.05. For the assay, 5 mL of the prepared ABTS solution was mixed with 0.1 mL of phycoerythrin at various concentrations (100, 250, 500, 750, and 1000 µg). The final absorbance was measured at 743 nm using a UV/ Vis spectrophotometer.

### In vitro anticancer activity of phycoerythrin

# Cell culture

The human lung cancer cell line (A549) was purchased from the National Centre for Cell Science (NCCS), Pune, and cultured in liquid Dulbecco's Modified Eagle Medium (DMEM) (Sigma, St. Louis, MO, USA) supplemented with Fetal Bovine Serum (FBS) 10% (v/v) (Biochrom, Berlin, Germany), penicillin 100 µg/mL, and streptomycin sulphate 100 µg/mL. The cells were maintained in an atmosphere of 5% $CO_2$ and 100% relative humidity at 37°C.

# MTT assay for cell cytotoxicity

The MTT [3-(4,5-dimethylthiazol-2-yl)-2,5-diphentyltetrazoliumbromide] assay was performed to evaluate the *in vitro* cytotoxicity of phycoerythrin on A549 cells, as described in [29]. Cultured A549 cells were harvested by trypsinization and collected into a 15 mL tube. The cells were then plated into a 96-well tissue culture plate at a density of $1 \times 10^5$ cells $mL^{-1}$ at the rate of 200 µL $well^{-1}$ in DMEM media with 10% FBS and 1% antibiotic solution for 24–48 h at 37°C. After incubation, the medium was replaced with serum-free DMEM, and wells were rinsed with sterile Phosphate Buffer Saline (PBS) and treated with various doses of phycoerythrin. Each sample was performed in triplicate, and the cells were cultured for 24 h at 37°C in a humidified 5% $CO_2$ incubator. Following, MTT (20 µL at 5 mg $mL^{-1}$) was added to each well after the incubation period, and the cells were incubated for another 2–4 h until purple precipitates were visible under an inverted microscope observation. Finally, the medium was aspirated within the wells together with MTT (220 µL) and rinsed with 200 µL of 1x PBS. The formazan crystals were dissolved by adding 100 µL of Dimethylsulfoxide (DMSO) to each well, and the plate was gently agitated for 5 min. Absorbance at 570 nm was measured using a microplate reader (Thermo Fisher Scientific, USA), and the percentage cell viability and $IC_{50}$ values were calculated using GraphPad Prism 6.0 software (USA).

# Apoptosis assay

A549 cells were planted at a density of $5\times10^5$ cells $mL^{-1}$ in a 96-well tissue culture plate in DMEM media with 10% FBS and 1% antibiotic solution for 24–48 h at 7°C. After incubation, the medium was replaced with serum-free DMEM, and wells were rinsed with PBS before being treated with 44.33 µg $mL^{-1}$ of phycoerythrin. Then, the plate was incubated at 37°C in a 5% $CO_2$ incubator for 24 h. Following the incubation, 10 µL Alexa Fluor and 10 µL propidium iodide were added to the wells, gently mixed, and incubated for 15 min. Subsequently, 400 µL of 1x Annexin binding buffer was added and gently mixed. The plate was centrifuged at 800 rpm for 2 min, and the cells were inspected using a fluorescence microscope with a fluorescent filter within 1 h [30].

# Computational analysis

# Target preprocessing

In the present study, the multitargeted proteins were chosen for the antimicrobial activity as Spore coat polysaccharide biosynthesis protein [PDB Id 1H7L], *Staphylococcus aureus* tyrosyl-tRNA synthetase [PDB id 1JIJ], Isoleucyl-tRNA synthetase [PDB ID QU3], Transcriptional regulator qacR [PDB ID 1RKW], HTH-Type Transcriptional Regulator MgrA [PDB ID 2BV6], YcgJ protein from *Bacillus subtilis* [PDB ID 2GLU], Dihydropteroate synthase [PDB ID 2VEG], Processed Glycerol Phosphate Lipoteichoic Acid Synthase 2 [PDB ID 2W8D], DNA Gyrase Subunit B, DNA Gyrase Subunit A [PDB ID 2XCT], DNA topoisomerase 4 subunit A [PDB ID 3RAE], Dihydrofolate reductase [PDB ID 3SRW], Penicillin-binding protein 3 [PDB ID 3VSL], Transcriptional regulator MvfR [PDB ID 4JVC] subjected for the molecular docking studies. These multitargeted proteins were retrieved from the Protein Data Bank (PDB). The preprocessing steps involved assigning bond orders, adding hydrogens, creating zero-order bonds to metals and disulfide bonds, converting seleno-methionines to methionine, and filling missing side chains using the Protein Preparation Wizard of the Maestro platform. The structures were then refined by optimizing hydrogen bonds and minimizing the structures using the OPLS4 force field (Maestro, Schrödinger 2021-2, NY, USA).

# Molecular docking

The flexible ligand docking parameter was enabled via Glide's XP (extra precision) function, and the target proteins and ligand molecules were docked using Maestro's Glide docking module. We determined the optimistic pose of the ligand-protein complex molecule by examining the interaction between the ligand and protein during docking using the XP pose viewer. We used the ligand interaction module to acquire the 2D interaction diagram. We subsequently analyzed the acquired XP pose to investigate the binding interactions of ligand molecules with the target protein [31, 32].

# Ligand preparation

The compound extracted from *K. alvarezii*, including (1,2-Benzisothiazol-3-amine, 2-Ethylacridine, 2,4-Dimethylbenzo[h]quinoline, 2-bromobutyloxychalcone), has been analyzed and profiled using GC-MS. We subsequently examined the 3D structures of the resultant compounds, retrieving them in the 3D structure data file format from the PubChem databases. We employed the LigPrep module to preprocess

the structures, using the OPLS4 force field to minimize energy and generate 32 different stereoisomeric and tautomeric states (Schrödinger Release 2021-2: LigPrep, Schrödinger, LLC, NY, 2021).

# Statistical analysis

The differences in the measured mean values between the triplicate observations were assessed for statistical significance using the student's two-tailed t test. A *p* value less than 0.05 was deemed significant.

## Results and discussion

*K. alvarezii* holds significant importance as a red macroalga due to its bioactive compounds, which hold significant therapeutic potential. Different fields have utilized their diverse, unique, biologically active substances. The evaluation focused on the antioxidant, antimicrobial, and anticancer properties of the extract from *K. alvarezii*. We conducted a chromatographic examination of its phycoerythrin pigment to gain a deeper understanding of the metabolic constituents involved.

# Extraction and purification of phycoerythrin pigment

Phycoerythrin was successfully extracted from microalgae using cell disruption methods such as sonication, mechanical maceration, and lysozyme treatments [21]. The centrifuged phycoerythrin pigment extracted from a *K. alvarezii* exhibited a red color. The purification and recovery involved four steps. The purity ratio of phycoerythrin, successively with ammonium sulfate (151.24 μg $mL^{-1}$, purity 2.24, recovery 74%) dialysis (338.71 μg $mL^{-1}$, purity 3.39, recovery 35%), and column chromatography yielded highest concentration and purity (554.12 μg $mL^{-1}$, purity 5.63, recovery 11%) when compared to crude pigment were reported in Table 1. *K. alvarezii* phycoerythrin was found to have a protein content of 69.84%. Similar findings were seen by previous researchers [33, 34]. The purification of R-phycoerythrin from the crude extract of *Gracilaria gracilis* was achieved using a one-step chromatographic method with a phosphate buffer of 20 mM at pH 7.1 [35], resulting in a high purity index, with an A565/A280 ratio of 3.25. This was accomplished through DEAE Sepharose fast flow column on anion-exchange chromatography, utilizing the fraction obtained at 200 mM NaCl. Compared to this study, our sequential purification process improves both phycoerythrin purity and concentration. Still, there is a trade-off between purity and recovery, with significant losses arising at each stage. Further, process optimization may be necessary to balance recovery efficacy with required purity levels. The selection of the appropriate cell disruption strategy significantly influences the recuperation of the entire process. Gel filtration expanded bed absorption chromatography, hydroxyapatite chromatography, and ion exchange chromatography are among the chromatographic technologies employed for purification.

Table 1
Phycoerythrin pigment purification and recovery steps

| Step | Volume (mL) | PE (μg $mL^{-1}$) | Purity (A620/A280) | Recovery (%) |
|---|---|---|---|---|
| Crude pigment | 100 | 78.43 | 0.95 | 100 |
| Ammonium sulfate precipitation of pigment | 15 | 151.24 | 2.24 | 74 |
| Dialysis of pigment | 10 | 338.71 | 3.39 | 35 |
| Sephadex G-100 Column chromatography of pigment | 5 | 554.12 | 5.63 | 11 |

# Characterization of phycoerythrin

# FT-IR analysis

The phycoerythrin bond and functional group analysis of FT-IR is shown in Fig. 1. The peak 3446.56 $cm^{-1}$ shows in O–H stretch and H–bonded stretching vibration presence of alcohols and phenols. The peak 3130.25 $cm^{-1}$ was present in the O–H stretching vibration functional group of carboxylic acids. The peak was 2920.99 $cm^{-1}$ C–H stretching vibration presence of alkanes. The peak 1719.42 $cm^{-1}$ C = O stretching vibration presence of alpha, beta–unsaturated esters. The peak 1610.45 $cm^{-1}$, 1528.48 $cm^{-1}$ and 1443.62 $cm^{-1}$ C–C stretch (in–ring) presence of aromatics. The peak 1383.83 $cm^{-1}$, 1264.25 $cm^{-1}$, 1139.85 $cm^{-1}$ and 1056.92 $cm^{-1}$ C–O stretch presence of alcohols, carboxylic acids, esters, ethers. The peak 994.24 $cm^{-1}$, 951.81 $cm^{-1}$, 865.01 $cm^{-1}$, 816.80 $cm^{-1}$, 761.83 $cm^{-1}$ and 619.11 $cm^{-1}$ =C–H bend alkenes. The peak 535.21 $cm^{-1}$ C–Br stretching vibration presence of alkyl halides. The FT-IR spectra is used to examine functional groups or chemical bonds within a molecule of an interaction system; it is used to analyze the functional groups or chemical bonds present in that molecule. Prior to extraction, the spectra display the absorption bands of DES at 1472 $cm^{-1}$ and dialyzed R-PE at 1074 $cm^{-1}$. FT-IR analysis of C-phycoerythrin (CPE) showed significant changes in the amide III, indicating interactions within the side chains. The protein backbone, on the other hand, seemed to have stayed mostly the same [36].

# HPLC analysis

HPLC analysis of phycoerythrin showed in Fig. 2. The obtained peaks were 2.110 (kaempferitrin), 2.823 (γ- tocopherol), 3.060 (β-sitosterol) and 4.353 (corilagin). Similar types of compounds were detected in a rapid two-step chromatographic technique for the purification of B-phycoerythrin from *Porphyridium cruentum* (S.F.Gray) Nägeli is presented [37]. The separation of its α-, β-, and γ-subunits was successfully accomplished using a reversed-phase HPLC gradient semipreparative approach. This involved a C4 large-pore column, and a solvent system made up of 0.05% trifluoroacetic acid (TFA) in water and 0.05% TFA in acetonitrile.

# GC-MS analysis

GC-MS analysis of the phycoerythrin revealed the following compounds such as 16.832 (-2-bromobutyloxychalcone), 17.024 (2-Ethylacridine), 17.072 (1,2-Benzisothiazol-3-amine) and 17.148 (Benzo[h]quinoline, 2,4-dimethyl-) within the peaks shown in Fig. 3. According [38], researchers collected *Gracilaria corticata* from Mandapam and subsequently identified and characterized it using GC-MS. Researchers prepared and analyzed the methanol extract using GC-MS to identify the various bioactive compounds present in the seaweed. The analysis identified a variety of bioactive compounds, including undecane, 2-decyloxirane, methyl n-tridecanoate, n-hexadecanoic acid, eicosanoic acid, nonanoic acid, oleic acid, pentadecanoic acid, bicycle [3.2.1] oct-3-en-2-one, 3,8-dihydroxy-1-1methoxy-7-(7-methoxy-1, 3 benzodioxol-5-yl)-6-methyl-5, N-(5-chloro-2-hydroxyphenyl) dodecanamide, and cholesta-8,24-dien-3-ol, 4-methyl. This research work examined the bioactive compounds derived from the methanol extract of seaweed through GC-MS analysis, highlighting their significant antimicrobial and free radical scavenging activities.

# Antibacterial activity of phycoerythrin

The antibacterial activity of phycoerythrin (30 µg) was evaluated against seven clinical pathogens. The maximum zone of suppression was found on *Klebsiella oxytoca* (20 mm), followed by *Escherichia coli* (17 mm), and *Pseudomonas aeruginosa* (18 mm), though generally less effective than Ampicillin (50 µg), which exhibited inhibition zones of 17–23 mm shown in Table 2. Similarly [39], the phycoerythrin of Microchaetes has antibacterial activity against human pathogens. Increasing the concentrations of phycoerythrin to 0.1 mg $mL^{-1}$ resulted in a higher percentage of inhibition across all bacterial strains tested. The antibacterial action of macroalgae involves changing the permeability of pathogen cells. This alteration leads to the loss of macromolecules, disrupts membrane functions, and ultimately results in the destruction of the bacterial cells [40, 41]. Research has demonstrated the effectiveness of seaweeds such as *K. alvarezii, Kappaphycus striatum*, and *Ulva lactuca* L. with antagonistic effects against human pathogenic bacteria [42].

Table 2
Antibacterial activity of phycoerythrin

| S. No | Bacterial pathogens | Ampicillin 50 µg (mm) | Phycoerythrin 30 µg (mm) |
|---|---|---|---|
| 1 | *Bacillus subtilis* | 17 | 12 |
| 2 | *Escherichia coli* | 20 | 17 |
| 3 | *Klebsiella oxytoca* | 23 | 20 |
| 4 | *Proteus mirabilis* | 19 | 11 |
| 5 | *Pseudomonas aeruginosa* | 21 | 18 |
| 6 | *Staphylococcus aureus* | 21 | 13 |
| 7 | *Streptococcus pyogenes* | 18 | 15 |

# Antioxidant activity of phycoerythrin pigment

The phycoerythrin pigment showed a total antioxidant capacity of 73.27 ± 0.43%, reducing power of 71.09 ± 0.23%, hydrogen peroxide scavenging activity of 67.54 ± 0.41%. Also, it showed 58.13 ± 0.99% activity in the DPPH, and 61.92 ± 0.34% in the ABTS assay, portraying its antioxidant potential (Table 3). Previous studies also proved the antioxidant potential of phycoerythrin from multiple seaweed sources. According to [43], hydrophilic PBPs from red macroalgae, have antioxidant activity against free radicals and selenium *in vitro* and *in vivo*. According to [44], phycoerythrin has antioxidant, anti-inflammatory, and hepatoprotective effects that are advantageous to human health. Algal antioxidants are divided into two types [45]. The water-soluble antioxidants include vitamins, PBPs, and polyphenols, while the fat-soluble antioxidants consist of carotenoids and tocopherol. The scavenging amount of DPPH radical by purified phycoerythrin varied with concentration, showing a concentration-dependent relationship, with an $IC_{50}$ value of 0.043 mg $mL^{-1}$, in contrast to 0.031 mg $mL^{-1}$ for ascorbic acid [39]. This indicates that phycoerythrin serves as an effective free radical scavenger, exhibiting DPPH scavenging properties comparable to those of ascorbic acid. The scavenging percentage of the ABTS radical by natural phycoerythrin varies with concentration. Phycoerythrin exhibited an $IC_{50}$ of 0.023 mg $mL^{-1}$, in contrast to Standard Butylated Hydroxyl Toluene (BHT), which had an $IC_{50}$ of 0.031 mg $mL^{-1}$. Phycoerythrin exhibits comparable ABTS scavenging activities to BHT and serves as a potent free radical scavenger [39]. The radical scavenging capacity of extracts of *Nostoc linckia* at 5 mg $l^{-1}$ improved with increasing PBPs content [46]. PBPs inhibits the generation of reactive oxygen species and hence the risk of diseases including cancer, diabetes, inflammation, and neurological diseases [47].

Table 3
Percentage of *in vitro* antioxidant activity of phycoerythrin

| S. No | Antioxidant activity | Phycoerythrin |
|---|---|---|
| 1 | Total antioxidant capacity | 73. 27 ± 0.43% |
| 2 | Reducing power | 71.09 ± 0.23% |
| 3 | Hydrogen peroxide scavenging assay | 67.54 ± 0.41% |
| 4 | DPPH | 58.13 ± 0.99% |
| 5 | ABTS | 61.92 ± 0.34% |

# Anticancer action of phycoerythrin pigment

## Cytotoxicity of cells by MTT assay

This study utilized the MTT assay to investigate the ways phycoerythrin affects the growth of A549 cancer cells. The cells endured culture for a duration of 24 h across a range of phycoerythrin concentrations. The viability of the cells was assessed through the MTT assay following a 24-hour incubation period. The alterations in the morphology of human lung cancer cells were observed following treatment with varying concentrations of phycoerythrin, as detailed in Table 4. The test showed a clear relationship between dosage and the level of toxicity in A549 human lung cancer cells. The cell viability showed a decline from 91.24 ± 0.09% at a concentration of 50 µg $mL^{-1}$ to 46.36 ± 0.16% at 500 µg $mL^{-1}$. Significant reductions were also observed at 200 µg $mL^{-1}$ (74.29 ± 0.07%) and 400 µg $mL^{-1}$ (54.85 ± 0.11%), emphasizing its promise as a potential anticancer agent. The concentrations of phycoerythrin at 50 µg $mL^{-1}$ and 100 µg $mL^{-1}$ indicated the presence of viable human lung cancer cells. The concentration of 100 µg $mL^{-1}$ of phycoerythrin showed the existence of both viable and non-viable cells. The levels of phycoerythrin between 200 and 400 µg $mL^{-1}$ indicated a minimal count of visible cells (Fig. 4).

Table 4
Viability of human lung cancer cells on cytotoxicity of phycoerythrin

| S. No | Concentration (μg $mL^{-1}$) | Cell viability (%) |
|---|---|---|
| 1 | Control | 100 ± 0.02 |
| 2 | 50 | 91.24 ± 0.09 |
| 3 | 100 | 82.59 ± 0.12 |
| 4 | 200 | 74.29 ± 0.07 |
| 5 | 300 | 69.04 ± 0.14 |
| 6 | 400 | 54.85 ± 0.11 |
| 7 | 500 | 46.36 ± 0.16 |

Human lung cancer cells treated with phycoerythrin experience growth inhibition. The tested sample exhibited an $IC_{50}$ value of 131.7 μg $mL^{-1}$. Ultimately, as the concentration of phycoerythrin increased, the presence of the cell steadily reduced. It is important to note that phycoerythrin demonstrates a more potent effect against human lung cancer cells shown in Table 5. Similarly, the various solvent extracts of *Gracilaria edulis* were evaluated against cancer cell lines for their anti-proliferative capabilities [48]. The *G. edulis* ethyl acetate extract (GEEA) at a concentration of 100 μg $mL^{-1}$ demonstrated a notable and highly significant reduction in growth within the A549 lung cancer cell line model. Additionally, when assessing a control group against a GEEA extract-treated group at different dosages (40, 60, 80, and 100 μg $mL^{-1}$) after 48 h, a minimal level of LDH release was observed. The cell cytotoxicity assay [39], revealed that phycoerythrin extracted from Michrochaete acts as an anticancer agent in the Hep G2 cell line at specific doses (20–160 g $mL^{-1}$), demonstrating an $IC_{50}$ value of 105.77 g $mL^{-1}$. In a similar way, anticancer efficacy of *Gracilaria cortica* phycoerythrin was reported against the HepG2 cell line [49].

Table 5
Tested phycoerythrin shows $IC_{50}$ values

| Log (inhibitor) | Phycoerythrin (µg $mL^{-1}$) |
|---|---|
| **Best-fit values** | |
| $LogIC_{50}$ | 2.119 |
| HillSlope | -1.017 |
| $IC_{50}$ | 131.7 |
| **Std. Error** | |
| $LogIC_{50}$ | 0.05416 |
| HillSlope | 0.1334 |
| **95% Confidence Intervals** | |
| $LogIC_{50}$ | 2.008 to 2.230 |
| HillSlope | -1.290 to -0.7434 |
| $IC_{50}$ | 102.0 to 170.0 |
| **Goodness of Fit** | |
| Degrees of Freedom | 28 |
| R square | 0.8809 |
| Absolute sum of squares | 3584 |
| Sy.x | 11.31 |
| **Number of points** | |
| Analyzed | 30 |

# Phycoerythrin induces apoptosis in cancer cells

The evaluation of apoptotic cells involved staining phycoerythrin with human lung cancer cells, as illustrated in Fig. 5. The control cells exhibited the highest number of viable cells, as indicated by green-coloured fluorescence. The percentage of apoptotic cells that tested positive for Annexin V/PI in human lung cancer cells treated with varying dosages of phycoerythrin (203.4 µg $mL^{-1}$) increased in accordance with the dosage levels. Cells treated with fluorouracil demonstrated the presence of both viable and non-viable cells. In addition to identifying the morphological changes associated with apoptosis, we also assessed the apoptosis rate using the annexin V test. Annexin V has a strong and specific attraction for damaged and compromised plasma membranes, making apoptotic and necrotic cells stand out. The

recent study demonstrated that phycoerythrin-induced apoptotic cell death in A549 lung cancer cells. Cell apoptosis [50], refers to a form of programmed cell death that relies on energy. Caspase belongs to the family of enzymes known for their specificity to aspartic acid and homocysteine proteases. These enzymes play a crucial role in degrading antiapoptotic proteins, leading to the release of mitochondrial cytochrome C.

## Molecular docking analysis

Computational biology combines computational techniques with biological systems to tackle disease-related challenges. Virtual screening, a key tool, reduces drug development costs and time by predicting receptor-ligand binding and affinities through docking and scoring. Molecular docking enhances drug discovery by accurately identifying ligand orientations in protein binding sites and predicting interaction strengths, significantly advancing the field [32]. By utilizing molecular docking, targeting the presence of antibacterial proteins in these compounds for the first time with the *K. alvarezii* extracted bioactive compounds. The 13 antibacterial multitarget proteins were docked with 4 compounds detected in GC-MS analysis of the phycoerythrin, revealing that a lower docking score corresponds to higher binding affinity (Table 6; Fig. 7–19). Molecular docking of K. alvarezii-derived compounds revealed significant binding affinities with 13 antibacterial target proteins. Among the results, the protein DNA gyrase subunits A (GyrA) and B (GyrB) showed a binding score of -1.13 kcal/mol with 1,2-Benzisothiazol-3-amine. *Staphylococcus aureus* tyrosyl-tRNA synthetase protein scored − 2.86 kcal/mol with 1,2-Benzisothiazol-3-amine, while dihydropteroate synthase and transcriptional regulator qacR scored − 1.17 kcal/mol and − 1.21 kcal/mol, respectively, with 2-bromobutyloxychalcone. Penicillin-binding protein 3 (-1.41 kcal/mol), DNA topoisomerase 4 subunit A (-1.66 kcal/mol), and isoleucyl-tRNA synthetase (-3.10 kcal/mol) also showed strong interactions with 1,2-Benzisothiazol-3-amine. Other substantial interactions included HTH-type transcriptional regulator MgrA (-2.39 kcal/mol) and processed glycerol phosphate lipoteichoic acid synthase 2 (-3.51 kcal/mol) with 2,4-dimethylbenzo[h]quinoline, and YcgJ protein from *Bacillus subtilis* (-2.52 kcal/mol) with 2-bromobutyloxychalcone. Particularly, transcriptional regulator MvfR (-4.88 kcal/mol) interacted strongly with 1,2-Benzisothiazol-3-amine, and dihydrofolate reductase exhibited the highest binding affinity (-5.24 kcal/mol) with 2-ethylacridine. In general, 1,2-Benzisothiazol-3-amine and 2-bromobutyloxychalcone demonstrated strong interactions with multiple targets, while 2-ethylacridine showed the highest affinity with dihydrofolate reductase (-5.24 kcal/mol), emerged as the most potent compound.

Table 6
The molecular docking of the antimicrobial target proteins with the compounds

| Compound ID | Compound Name | Amino acid Interaction | Bond Length | Glide Score | Glide Energy |
|---|---|---|---|---|---|
| 1H7L - Spore coat polysaccharide biosynthesis protein SpsA | | | | | |
| 89966 | 1,2-Benzisothiazol-3-amine | HIS 159,<br>TYR 77. | [2.03]; [4.21, 3.70]. | -3.44 | -20.03 |
| 610161 | 2-Ethylacridine | PHE 233,<br>TYR 11,<br>TYR 77,<br>ARG 76. | [5.03]; [5.49];<br>[5.21, 5.84, 5.45]; [5.31]. | -3.90 | -24.14 |
| 610182 | 2,4-Dimethylbenzo[h]quinoline | ARG 76,<br>LEU 80. | [5.17]; [4.81]. | -4.95 | -27.35 |
| 91733949 | 2-bromobutyloxychalcone | THR 9,<br>ASP 99,<br>TYR 11,<br>ARG 76,<br>TYR 77. | [2.21];<br>[2.50, 2.59];<br>[5.55]; [5.18, 5.12]; [5.24]. | -4.63 | -37.07 |
| 1JIJ - *Staphylococcus aureus* tyrosyl-tRNA synthetase | | | | | |
| 89966 | 1,2-Benzisothiazol-3-amine | ALA 39,<br>ASP 40. | [4.38,4.23]; [2.74,1.94]. | -2.86 | -22.97 |
| 610161 | 2-Ethylacridine | ASP 195,<br>TYR 36,<br>CYS37,<br>GLY 192. | [4.51]; [5.31];<br>[2.94,5.17,5.04];<br>[2.80,2.92]. | -3.82 | -27.65 |
| 610182 | 2,4-Dimethylbenzo[h]quinoline | ASP 80,<br>TYR 36,<br>LEU 70,<br>CYS 37. | [4.45]; [5.26];<br>[3.81]; [4.05]. | -3.94 | -32.71 |
| 91733949 | 2-bromobutyloxychalcone | LEU 70,<br>GLN 190, | [4.80]; [2.08];<br>[4.93]; [3.08]; | -4.79 | -46.30 |

| Compound ID | Compound Name | Amino acid Interaction | Bond Length | Glide Score | Glide Energy |
|---|---|---|---|---|---|
| | | CYS 37,<br>GLY 193,<br>GLN196. | [2.77]. | | |
| 1QU3 - Isoleucyl-tRNA synthetase (IleRS) | | | | | |
| 89966 | 1,2-Benzisothiazol-3-amine | GLU 554. | [1.73]. | -3.10 | -22.76 |
| 610161 | 2-Ethylacridine | GLY 554,<br>TRP 562,<br>TRP 528, | [1.64]; [5.41, 4.94]; [4.78]. | -7.92 | -35.62 |
| 610182 | 2,4-Dimethylbenzo[h]quinoline | PRO 56,<br>GLU 554,<br>TRP 562,<br>ASP 557,<br>HIS 64. | [5.26]; [2.41];<br>[5.97, 5.13];<br>[4.46, 5.22];<br>[5.47]. | -6.25 | -30.45 |
| 91733949 | 2-bromobutyloxychalcone | TRP 528,<br>GLY 555,<br>GLU 554,<br>ASN 70,<br>HIS 67,<br>PRO 57. | [5.97]; [2.14];<br>[2.84]; [2.68];<br>[4.24]; [5.37]. | -4.71 | -40.99 |
| 1RKW - Transcriptional regulator qacR | | | | | |
| 89966 | 1,2-Benzisothiazol-3-amine | HIS 42,<br>GLU 52. | [1.93];<br>[3.67, 3.49]. | -1.98 | -16.57 |
| 610161 | 2-Ethylacridine | GLU 52,<br>LYS 115,<br>LYS 118,<br>LEU 119. | [4.52]; [4.21, 4.58, 5.17, 4.00, 4.21];<br>[4.31];<br>[5.16]. | -2.95 | -31.49 |
| 610182 | 2,4-Dimethylbenzo[h]quinoline | LYS 115,<br>GLU 52. | [4.24]; [4.40, 3.62, 3.70]. | -1.80 | -19.45 |

| Compound ID | Compound Name | Amino acid Interaction | Bond Length | Glide Score | Glide Energy |
|---|---|---|---|---|---|
| 91733949 | 2-bromobutyloxychalcone | ASN 55,<br>LYS 118,<br>LYS 115. | [2.32]; [4.36];<br>[3.08,4.92]. | -1.21 | -26.36 |
| 2BV6 - HTH-type transcriptional regulator MgrA | | | | | |
| 89966 | 1,2-Benzisothiazol-3-amine | ALA 63,<br>LEU 62,<br>LEU 42,<br>PRO 39,<br>TYR 38. | [2.19, 4.96];<br>[2.81, 4.48];<br>[5.42]; [4.90];<br>[5.50]. | -3.06 | -17.13 |
| 610161 | 2-Ethylacridine | LEU 42,<br>PRO 39,<br>LEU 62,<br>ALA 63. | [4.91]; [4.84];<br>[5.01]; [2.26, 5.12, 5.03]. | -2.75 | -20.26 |
| 610182 | 2,4-Dimethylbenzo[h]quinoline | ALA 63,<br>LEU 62,<br>LEU 42,<br>PRO 39,<br>TYR 38. | [5.10, 4.93, 3.95, 2.25]; [5.37];<br>[5.13]; [5.28, 4.88]; [5.30] | -2.39 | -19.83 |
| 91733949 | 2-bromobutyloxychalcone | VAL 116,<br>TYR 38,<br>GLN 19,<br>LEU 134,<br>PHE 41,<br>LEU 42. | [4.94]; [3.00];<br>[2.05, 2.98];<br>[4.23]; [4.32];<br>[4.99]. | -3.89 | -30.05 |
| 2GLU - YcgJ protein from *Bacillus subtilis* | | | | | |
| 89966 | 1,2-Benzisothiazol-3-amine | PRO 119,<br>TYR 117. | [5.12]; [2.08]. | -2.85 | -15.11 |
| 610161 | 2-Ethylacridine | LEU 145, | [5.27]; [4.96]; | -2.61 | -18.78 |

| Compound ID | Compound Name | Amino acid Interaction | Bond Length | Glide Score | Glide Energy |
|---|---|---|---|---|---|
| | | LEU 167,<br>PRO 168,<br>GLN 149. | [5.12, 4.86];<br>[2.14, 2.82]. | | |
| 610182 | 2,4-Dimethylbenzo[h]quinoline | TYR 159,<br>GLN 149,<br>LEU 145,<br>GLU 120. | [5.35]; [1.94];<br>[4.48, 5.09];<br>[4.21, 4.48]. | -3.35 | -20.95 |
| 91733949 | 2-bromobutyloxychalcone | PRO 168,<br>GLU 120,<br>PRO 119. | [4.42]; [2.90];<br>[2.57, 4.82]. | -2.52 | -30.91 |
| 2VEG - Dihydropteroate synthase | | | | | |
| 89966 | 1,2-Benzisothiazol-3-amine | ASP 221,<br>GLN 276,<br>ARG 275,<br>LLE 272. | [1.92]; [3.06];<br>[4.15, 4.13];<br>[5.42]. | -3.22 | -16.19 |
| 610161 | 2-Ethylacridine | ARG 275,<br>LLE 272,<br>ASP 221. | [3.88, 5.36, 3.95];<br>[4.85]; [2.07]. | -4.24 | -2312 |
| 610182 | 2,4-Dimethylbenzo[h]quinoline | ARG 275,<br>ASP 221. | [4.39, 4.59];<br>[3.87, 3.68]. | -2.71 | -23.28 |
| 91733949 | 2-bromobutyloxychalcone | ARG 275. | [5.45, 4.01]. | -1.17 | -26.44 |
| 2W8D - Processed glycerol phosphate lipoteichoic acid synthase 2 | | | | | |
| 89966 | 1,2-Benzisothiazol-3-amine | TRP 350,<br>ASN 478,<br>HIS 479,<br>PHE 413. | [5.23, 4.85, 3.53, 4.21]; [3.02];<br>[2.45]; [5.04]. | -4.05 | -21.07 |
| 610161 | 2-Ethylacridine | TRP 350,<br>ASN 478, | [4.97, 4.03, 5.01, 3.78, 4.46]; [3.10];<br>[4.79, 4.07]. | -4.58 | -24.35 |

| Compound ID | Compound Name | Amino acid Interaction | Bond Length | Glide Score | Glide Energy |
|---|---|---|---|---|---|
| | | HIS 479. | | | |
| 610182 | 2,4-Dimethylbenzo[h]quinoline | HIS 479, PHE 349, ASN 478, TYR 380, PHE 413, TRP 350. | [4.31]; [4.74]; [2.68]; [5.09]; [504]; [4.19, 5.08, 5.15, 4.87, 4.48, 3.44]. | -3.51 | -18.95 |
| 91733949 | 2-bromobutyloxychalcone | TPO 297, TRP 350, TYR 380, PHE 349, ASN 478, PHE 413. | [4.02]; [2.27]; [5.64]; [4.32]; [2.07]; [4.76]. | -7.16 | -36.62 |
| 2XCT - DNA gyrase subunit B, DNA gyrase subunit A | | | | | |
| 89966 | 1,2-Benzisothiazol-3-amine | LLE 1452, LYS 1375, ALA 1378, GLU 1382, LEU 1449. | [5.16]; [3.55, 4.20]; [5.32]; [1.92]; [5.07]. | -0.97 | -11.96 |
| 610161 | 2-Ethylacridine | GLU 1382, LEU 1449, LYS 135, LLE 1452. | [1.52]; [5.13, 4.76]; [3.97]; [4.17]. | -2.69 | -27.77 |
| 610182 | 2,4-Dimethylbenzo[h]quinoline | LLE 1452, LYS 1375, ALA 1378, LEU 1449, GLU 1382. | [5.16]; [5.14]; [3.65]; [4.97, 4.57]; [5.51]. | -2.86 | -22.49 |

| Compound ID | Compound Name | Amino acid Interaction | Bond Length | Glide Score | Glide Energy |
|---|---|---|---|---|---|
| 91733949 | 2-bromobutyloxychalcone | LLE 1452,<br>LEU 1449,<br>ASN 474. | [4.97]; [5.28, 5.38]; [2.11]. | -1.13 | -26.97 |
| 3RAE - DNA topoisomerase 4 subunit A | | | | | |
| 89966 | 1,2-Benzisothiazol-3-amine | PRO 113,<br>ARG 117,<br>MET 116,<br>ALA 115. | [2.95]; [4.72];<br>[5.45]; [4.13, 3.91]. | -1.66 | -24.21 |
| 610161 | 2-Ethylacridine | PRO 112,<br>TYR 82,<br>ALA 115,<br>MET 116. | [5.02]; [4.42];<br>[4.68]; [4.39]. | -2.95 | -31.49 |
| 610182 | 2,4-Dimethylbenzo[h]quinoline | ASP 83,<br>MET 116,<br>ALA 115. | [4.01]; [5.52];<br>[4.71, 4.65]. | -3.64 | -29.51 |
| 91733949 | 2-bromobutyloxychalcone | ALLA 115,<br>MET 116,<br>ARG 117. | [4.76]; [5.30];<br>[2.40]. | -2.79 | -34.49 |
| 3SRW - Dihydrofolate reductase | | | | | |
| 89966 | 1,2-Benzisothiazol-3-amine | LLE 15,<br>LEU 21,<br>ALA 8,<br>PHE 93. | [2.07]; [5.15, 5.43]; [2.14, 2.27,5.13];<br>[5.18, 5.63]. | -6.08 | -22.26 |
| 610161 | 2-Ethylacridine | LEU 21,<br>LEU 29,<br>PHE 93,<br>LLE 15. | [4.46, 4.35]; [5.14]; [5.28];<br>[4.70]. | -5.24 | -278994 |

| Compound ID | Compound Name | Amino acid Interaction | Bond Length | Glide Score | Glide Energy |
|---|---|---|---|---|---|
| 610182 | 2,4-Dimethylbenzo[h]quinoline | PHE 93,<br>LLE 15,<br>LEU 21. | [4.87]; [5.36];<br>[4.51, 5.10]. | -5.63 | -29.9 |
| 91733949 | 2-bromobutyloxychalcone | VAL 132,<br>VAL 17,<br>LLE 15,<br>ALA 8,<br>LEU 21,<br>ASN 19. | [5.43]; [2.61];<br>[5.28]; [1.99, 5.32]; [4.84];<br>[2.59]. | -7.13 | -41.79 |
| 3VSL - Penicillin-binding protein 3 | | | | | |
| 89966 | 1,2-Benzisothiazol-3-amine | ASN 501,<br>VAL 493,<br>LYS 494. | [1.94]; [5.34, 3.25]; [4.87, 3.98, 4.27]. | -1.41 | -19.70 |
| 610161 | 2-Ethylacridine | LYS 494,<br>ASN 501,<br>PRO 500,<br>TYR 278. | [4.91, 3.07, 2.81]; [3.01, 2.59]; [5.20]<br>[4.97]. | -3.22 | -24.34 |
| 610182 | 2,4-Dimethylbenzo[h]quinoline | LYS 494,<br>ASN 501,<br>PRO 500. | [4.76, 5.38];<br>[2.76, 2.15];<br>[5.30, 5.45]. | -2.75 | -22.93 |
| 91733949 | 2-bromobutyloxychalcone | TYR 278,<br>LYS 494,<br>HIS 259,<br>LEU 576. | [4.61]; [1.98];<br>[5.56]; [5.06]. | -4.66 | -35.39 |
| 4JVC - Transcriptional regulator MvfR | | | | | |
| 89966 | 1,2-Benzisothiazol-3-amine | LEU 197,<br>GLN 194,<br>ARG 209, | [2.63]; [2.90];<br>[2.07]; [2.58];<br>[2.81, 3.98]; | -4.88 | -27.06 |

| Compound ID | Compound Name | Amino acid Interaction | Bond Length | Glide Score | Glide Energy |
|---|---|---|---|---|---|
| | | LEU 207,<br>LLE 236,<br>LEU 208. | [4.77, 5.14]. | | |
| 610161 | 2-Ethylacridine | LLE 236,<br>ALA 102,<br>ALA 168,<br>LLE 149,<br>LEU 208. | [4.92, 3.87, 4.17]; [4.27];<br>[4.16, 3.25];<br>[4.95, 4.05];<br>[4.99, 4.94]. | -6.71 | -19.70 |
| 610182 | 2,4-Dimethylbenzo[h]quinoline | LLE 149,<br>ALA 168,<br>LLE 236,<br>VAL 211,<br>LEU 208. | [5.32]; [4.52];<br>[4.54, 3.98, 4.12, 5.45]; [5.48];<br>[4.80,4.87]. | -6.71 | -28.29 |
| 91733949 | 2-bromobutyloxychalcone | ALA 102,<br>PRO 238,<br>ALA 168,<br>LLE 236,<br>LLE 149,<br>LEU 208,<br>ARG 209. | [4.37]; [4.96]<br>[3.22]; [5.29, 2.87]; [4.31];<br>[5.14]; [4.02]; | -7.26 | -34.37 |

# Conclusions

The scope of the present paper was to assess the potential of seaweed as a novel source for marine pharmaceuticals. This study successfully isolated and purified phycoerythrin from *K. alvarezii* using a process that included ammonium sulfate precipitation, dialysis, and column chromatography. In the FT-IR test, many different functional groups were found. In the HPLC test, bioactive compounds such as kaempferitrin, β-sitosterol, and 2-bromobutyloxychalcone were found. The antioxidant activity of phycoerythrin was very high, with a total antioxidant capacity of 73.27% and strong scavenging abilities in the DPPH and ABTS tests. Its antibacterial activity was most effective against *K. oxytoca* (20 mm) and moderately active against other pathogens. MTT assays verified that cytotoxicity against A549 human lung cancer cells was dose-dependent, and Annexin V/PI staining revealed increased apoptotic activity.

Molecular docking further emphasized the potential of phycoerythrin as a natural source of bioactive compounds for therapeutic applications, highlighting its potential in antimicrobial target protein interactions. The outcome of this study demonstrates the potential of the red seaweed *K. alvarezii* against cancer cell lines, supporting the way forward for the development of phycoerythrin as anti-cancer drug with pharmaceutical prospective.

# Clinical trial number

Not applicable

# Statement

We implemented all methods in accordance with pertinent regulations and guidelines. The authors have not conducted any experiments on humans or utilized human tissue samples. The ethics committee of the institute approved all experimental protocols and panelists involved in the study.

# Declarations

The authors declare that data supporting the findings of this study will be available from the corresponding author upon reasonable request.

### Clinical trial number

Not applicable

### Statement

We implemented all methods in accordance with pertinent regulations and guidelines. The authors have not conducted any experiments on humans or utilized human tissue samples. The ethics committee of the institute approved all experimental protocols and panelists involved in the study.

### Acknowledgement

Authors would like to express their gratitude to Ayya Nadar Janaki Ammal College, Tamil Nadu, for providing the necessary facilities to conduct this research, as well as the International Centre for Genetic Engineering and Biotechnology, New Delhi for their assistance with molecular docking. The authors extend their deep appreciation to Researchers Supporting Project number (RSPD2025R741), King Saud University, Riyadh, Saudi Arabia.

### Authors contributions

H.B., G.R.P. and D.P. conceived and designed the experiments. P.S. and S.S. drafted the main manuscript text. H.B., S.M., M.M., J.P. and P.M. conducted the extraction, GC-MS analysis, and antibacterial, antioxidant, and anticancer experiments. M.A., S.V. and P.S. carried out the molecular docking analyses.

D.P. and A.P. supervised the research project. F.U., H.O.E., M.N., A.A.F., M.A.R. and I.M.M. contributed to funding acquisition, manuscript review and editing, and project administration.


### Funding

Researchers Supporting Project number (RSPD2025R741), King Saud University.


### Ethics approval and consent to participate

Not applicable.

### Consent for publication

Not applicable.

### Competing interests

The authors declare no competing interests

### Additional information

Correspondenceand requests for materials should be addressed to D.P.

## References


1. Menaa F, Wijesinghe U, Thiripuranathar G, Althobaiti NA, Albalawi AE, Khan BA, et al. Marine algae-derived bioactive compounds: A new wave of nanodrugs? Mar Drugs. 2021;19:1–36.
2. Ahmed N, Sheikh MA, Ubaid M, Chauhan P, Kumar K, Choudhary S. Comprehensive exploration of marine algae diversity, bioactive compounds, health benefits, regulatory issues, and food and drug applications. Meas Food. 2024; 100163.
3. Banday AH, Azha N ul, Farooq R, Sheikh SA, Ganie MA, Parray MN, et al. Exploring the potential of marine natural products in drug development: A comprehensive review. Phytochem Lett. 2024;124–35.
4. Eladl SN, Elnabawy AM, Eltanahy EG. Recent biotechnological applications of value-added bioactive compounds from microalgae and seaweeds. Bot Stud. 2024;65.
5. Cupo A, Landi S, Morra S, Nuzzo G, Gallo C, Manzo E, et al. Autotrophic vs. Heterotrophic cultivation of the marine diatom *Cyclotella cryptica* for epa production. Mar Drugs. 2021;19:1–11.
6. Bora A, Thondi Rajan AS, Ponnuchamy K, Muthusamy G, Alagarsamy A. Microalgae to bioenergy production: Recent advances, influencing parameters, utilization of wastewater – A critical review. Sci Total Environ. 2024;174230.
7. Rudke AR, de Andrade CJ, Ferreira SRS. *Kappaphycus alvarezii* macroalgae: An unexplored and valuable biomass for green biorefinery conversion. Trends Food Sci Technol. 2020;214–24.

8. Solorzano-Chavez EG, Paz-Cedeno FR, Ezequiel de Oliveira L, Gelli VC, Monti R, Conceição de Oliveira S, et al. Evaluation of the *Kappaphycus alvarezii* growth under different environmental conditions and efficiency of the enzymatic hydrolysis of the residue generated in the carrageenan processing. Biomass and Bioenergy. 2019;105254.
9. Das D, Arulkumar A, Paramasivam S, Lopez-Santamarina A, del Carmen Mondragon A, Miranda Lopez JM. Phytochemical Constituents, Antimicrobial Properties and Bioactivity of Marine Red Seaweed (*Kappaphycus alvarezii*) and Seagrass (*Cymodocea serrulata*). Foods. 2023;12.
10. Gereniu CRN, Saravana PS, Getachew AT, Chun BS. Characteristics of functional materials recovered from Solomon Islands red seaweed (*Kappaphycus alvarezii*) using pressurized hot water extraction. J Appl Phycol. 2017;29:1609–21.
11. Sharma R, Mondal AS, Trivedi N. Anticancer potential of algae-derived metabolites: recent updates and breakthroughs. Futur J Pharm Sci. 2023;9.
12. Nunes A, Azevedo GZ, de Souza Dutra F, dos Santos BR, Schneider AR, Oliveira ER, et al. Uses and applications of the red seaweed *Kappaphycus alvarezii*: a systematic review. J Appl Phycol. 2024;:1–42.
13. Bray F, Laversanne M, Sung H, Ferlay J, Siegel RL, Soerjomataram I, et al. Global cancer statistics 2022: GLOBOCAN estimates of incidence and mortality worldwide for 36 cancers in 185 countries. CA Cancer J Clin. 2024;74:229–63.
14. Leiter A, Veluswamy RR, Wisnivesky JP. The global burden of lung cancer: current status and future trends. Nat Rev Clin Oncol. 2023;20:624–39.
15. Lanoix JP, Pluquet E, Lescure FX, Bentayeb H, Lecuyer E, Boutemy M, et al. Bacterial infection profiles in lung cancer patients with febrile neutropenia. BMC Infect Dis. 2011;11.
16. Ye M, Gu X, Han Y, Jin M, Ren T. Gram-negative bacteria facilitate tumor outgrowth and metastasis by promoting lipid synthesis in lung cancer patients. J Thorac Dis. 2016;8:1943–55.
17. Sun Y, Wen M, Liu Y, Wang Y, Jing P, Gu Z, et al. The human microbiome: A promising target for lung cancer treatment. Front Immunol. 2023;1–12.
18. Anand U, Dey A, Chandel AKS, Sanyal R, Mishra A, Pandey DK, et al. Cancer chemotherapy and beyond: Current status, drug candidates, associated risks and progress in targeted therapeutics. Genes Dis. 2023;10:1367–401.
19. Manohar M, Sharan V L, Joshy V A. Recent advances in in vitro and in vivo studies on *Kappaphycus alvarezii* and its derivatives. Nat Prod Res. 2024;1–14.
20. Uju, Dewi NPSUK, Santoso J, Setyaningsih I, Hardingtyas SD, Yopi. Extraction of phycoerythrin from *Kappaphycus alvarezii* seaweed using ultrasonication. IOP Conf Ser Earth Environ Sci. 2020;414.
21. Ulagesan S, Nam TJ, Choi YH. Extraction and purification of r-phycoerythrin alpha subunit from the marine red algae *Pyropia yezoensis* and its biological activities. Molecules. 2021;26.
22. Cotas J, Leandro A, Pacheco D, Gonçalves AMM, Pereira L. A comprehensive review of the nutraceutical and therapeutic applications of red seaweeds (Rhodophyta). Life. 2020;10.

23. Pugalendren S, Sarangam B, Rengasamy R. Extraction of R-Phycoerythrin from *Kappaphycus alvarezii* (Doty) Doty ex Silva and analyses of its physico-chemical properties. J Acad Ind Res. 2012;1:407.
24. Prieto P, Pineda M, Aguilar M. Spectrophotometric quantitation of antioxidant capacity through the formation of a phosphomolybdenum complex: Specific application to the determination of vitamin E. Anal Biochem. 1999;269:337–41.
25. Ramalingam V, Rajaram R. Enhanced antimicrobial, antioxidant and anticancer activity of *Rhizophora apiculata*: An experimental report. 3 Biotech. 2018;8.
26. Gantar M, Dhandayuthapani S, Rathinavelu A. Phycocyanin induces apoptosis and enhances the effect of topotecan on prostate cell line LNCaP. J Med Food. 2012;15:1091–5.
27. Ramalingam V, Rajaram R. Antioxidant activity of 1-hydroxy-1-norresistomycin derived from *Streptomyces variabilis* KP149559 and evaluation of its toxicity against zebra fish Danio rerio. RSC Adv. 2016;6:16615–23.
28. Re R, Nicoletta P, Anna P, Ananth P, Min Y, Catherine R-E. Antioxidant activity applying an improved ABTS radical cation decolorization assay. Free Radic Biol Med. 1999;26 (9-10):1231–7.
29. Mohan H, Ramalingam V, Lim JM, Lee SW, Kim J, Lee JH, et al. E-waste based graphene oxide/V2O5/Pt ternary composite: Enhanced visible light driven photocatalyst for anti-microbial and anti-cancer activity. Colloids Surfaces A Physicochem Eng Asp. 2020; 125469.
30. Ramalingam V, Raja S, Harshavardhan M. In situ one-step synthesis of polymer-functionalized palladium nanoparticles: An efficient anticancer agent against breast cancer. Dalt Trans. 2020;49:3510–8.
31. Leslie VA, Mohammed Alarjani K, Malaisamy A, Balasubramanian B. Bacteriocin producing microbes with bactericidal activity against multidrug resistant pathogens. J Infect Public Health. 2021;14:1802–9.
32. Malaisamy AK, Balasubramanian B, Tamilselvan PY, Sakthivel V, Venkatachalapathi S, Bhotla HK. Probing marine macroalgal phlorotannins as an antibacterial candidate against *Salmonella typhi*: Molecular docking and dynamics simulation approach. Curr Plant Biol. 2024;100418.
33. Sharmila G, Nikitha VS, Ilaiyarasi S, Dhivya K, Rajasekar V, Kumar NM, et al. Ultrasound assisted extraction of total phenolics from *Cassia auriculata* leaves and evaluation of its antioxidant activities. Ind Crops Prod. 2016;84:13–21.
34. Benavides J, Rito-Palomares M. Bioprocess intensification: A potential aqueous two-phase process for the primary recovery of B-phycoerythrin from *Porphyridium cruentum*. J Chromatogr B Anal Technol Biomed Life Sci. 2004;807:33–8.
35. Nguyen HPT, Morançais M, Déléris P, Fleurence J, Nguyen-Le CT, Vo KH, et al. Purification of R-phycoerythrin from a marine macroalga *Gracilaria gracilis* by anion-exchange chromatography. J Appl Phycol. 2020;32:553–61.
36. Ghosh T, Vyas A, Bhayani K, Mishra S. C-Phycoerythrin as a Colorimetric and Fluorometric Probe for the Sensitive, Selective and Quantitative Detection of Cu2+ in Aqueous Samples. J Fluoresc.

2018;28:671–80.

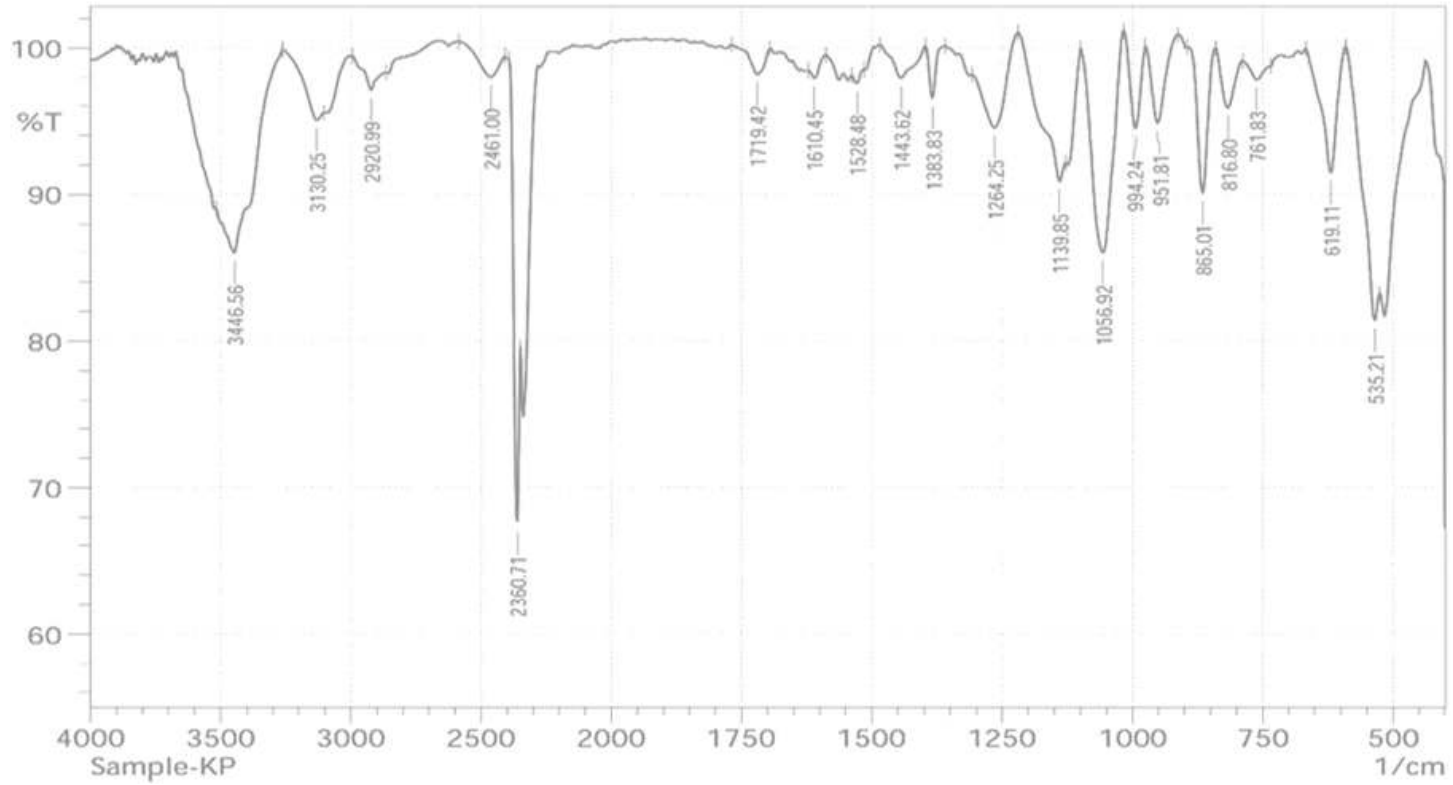
37. Bermejo R, Talavera EM, Alvarez-Pez JM. Chromatographic purification and characterization of B-phycoerythrin from *Porphyridium cruentum* - Semipreparative high-performance liquid chromatographic separation and characterization of its subunits. J Chromatogr A. 2001;917:135–45.
38. Ragunathan V, Pandurangan J, Ramakrishnan T. Gas Chromatography-mass spectrometry Analysis of Methanol Extracts from Marine Red Seaweed Gracilaria corticata. Pharmacogn J. 2019;11:547–54.
39. Hemlata, Afreen S, Fatma T. Extraction, purification and characterization of phycoerythrin from Michrochaete and its biological activities. Biocatal Agric Biotechnol. 2018;84–9.
40. Abu-Khudir R, Ismail GA, Diab T. Antimicrobial, Antioxidant, and Anti-Tumor Activities of *Sargassum linearifolium* and *Cystoseira crinita* from Egyptian Mediterranean Coast. Nutr Cancer. 2021;73:829–44.
41. El-Sheekh M, El Sabbagh S, Abd El Samea B. Control of Some Microbial Skin Diseases By Some Marine Algal Extract. J Agric Chem Biotechnol. 2016;7:67–74.
42. Sivakumar K, Kannappan S, Vijayakumar B. Molecular docking approaches of biomolecules extracted from red seaweed *Kappaphycus alvarezii* against hemolysin protein of bioluminescence disease-causing bacteria *Vibrio harveyi*. Algal Res. 2023;103207.
43. Punampalam R, Khoo KS, Sit NW. Evaluation of antioxidant properties of phycobiliproteins and phenolic compounds extracted from *Bangia atropurpurea*. Malaysian J Fundam Appl Sci. 2018;14:289–97.
44. Hsieh-Lo M, Castillo G, Ochoa-Becerra MA, Mojica L. Phycocyanin and phycoerythrin: Strategies to improve production yield and chemical stability. Algal Res. 2019;101600.
45. Ina A, Kamei Y. Vitamin B12, a chlorophyll-related analog to pheophytin a from marine brown algae, promotes neurite outgrowth and stimulates differentiation in PC12 cells. Cytotechnology. 2006;52:181–7.
46. Valuta A, Cepoi L, Rudi L, Bulhac I, Bourosh P, Bologa O. Phycobiliprotein accumulation in Cyanobacterium *Nostoc linckia* and modification of antioxidant activity. Ann Oradea Univ Biol Fascicle. 2015;21:13–9.
47. Li S, Ji L, Shi Q, Wu H, Fan J. Advances in the production of bioactive substances from marine unicellular microalgae *Porphyridium* spp. Bioresour Technol. 2019;292 June:122048.
48. Sakthivel R, Muniasamy S, Archunan G, Devi KP. *Gracilaria edulis* exhibit antiproliferative activity against human lung adenocarcinoma cell line A549 without causing adverse toxic effect *in vitro* and *in vivo*. Food Funct. 2016;7:1155–65.
49. Zandi K, Tajbakhsh S, Nabipour I, Rastian Z, Yousefi F, Sharafian S, et al. In vitro antitumor activity of *Gracilaria corticata* (a red alga) against jurkat and molt-4 human cancer cell lines. African J Biotechnol. 2010;9:6787–90.
50. Logue SE, Martin SJ. Caspase activation cascades in apoptosis. Biochem Soc Trans. 2008;36:1–9.

# Figures



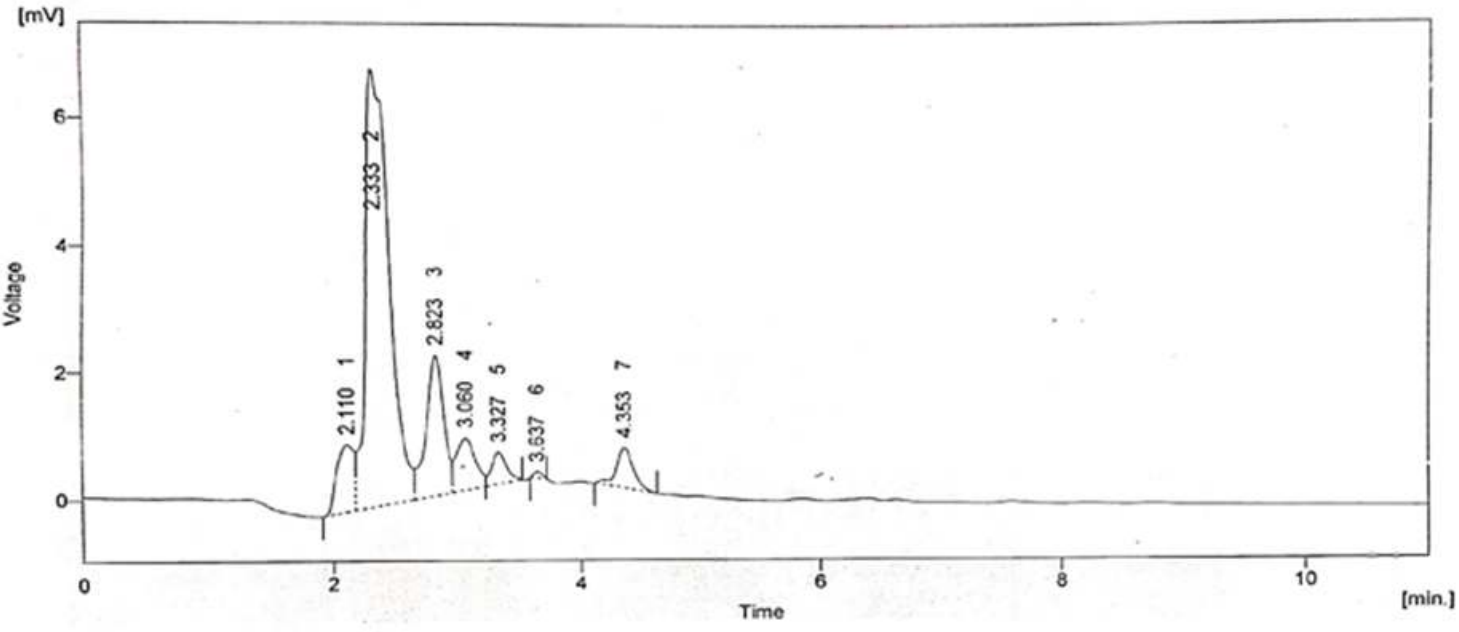
**Figure 1**

*Kappaphycus alvarezii*



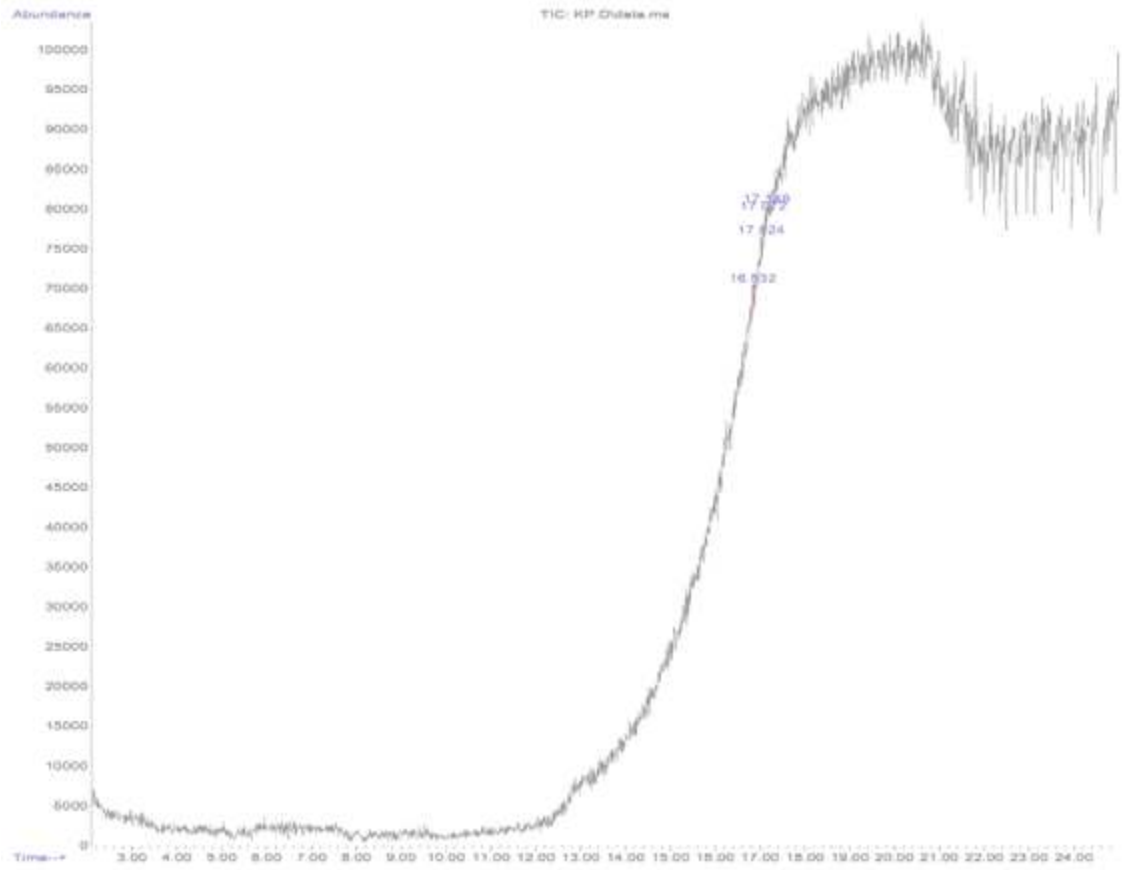

## Figure 2

FT-IR analysis of phycoerythrin



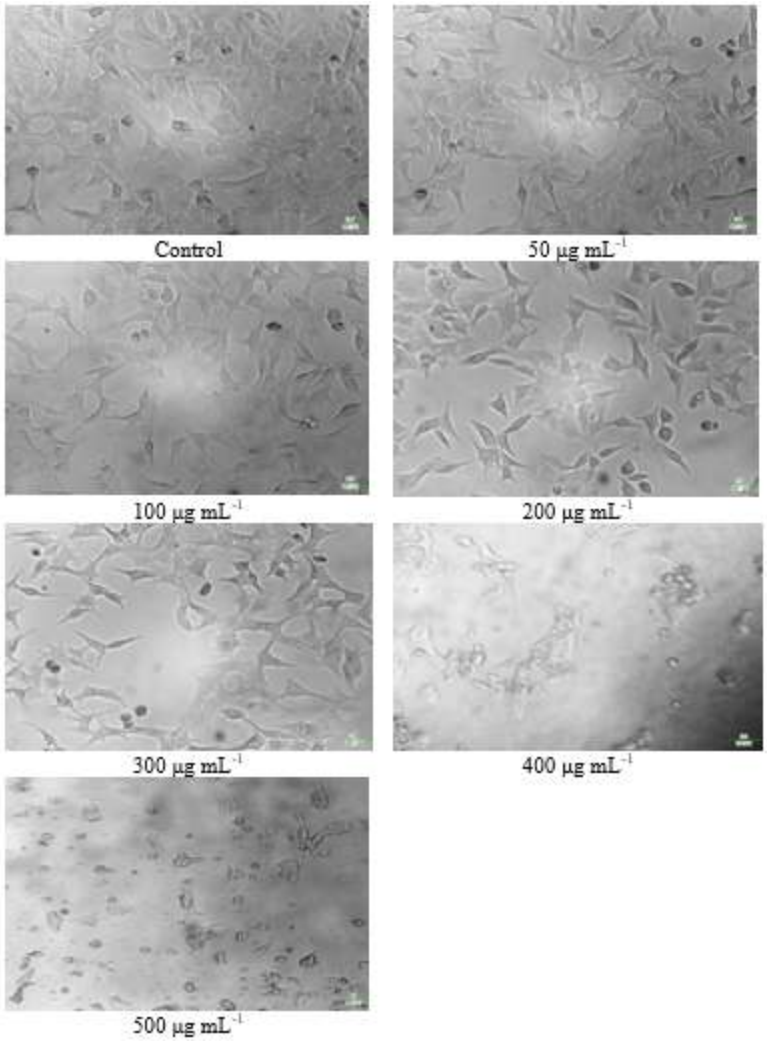

## Figure 3

HPLC analysis of phycoerythrin



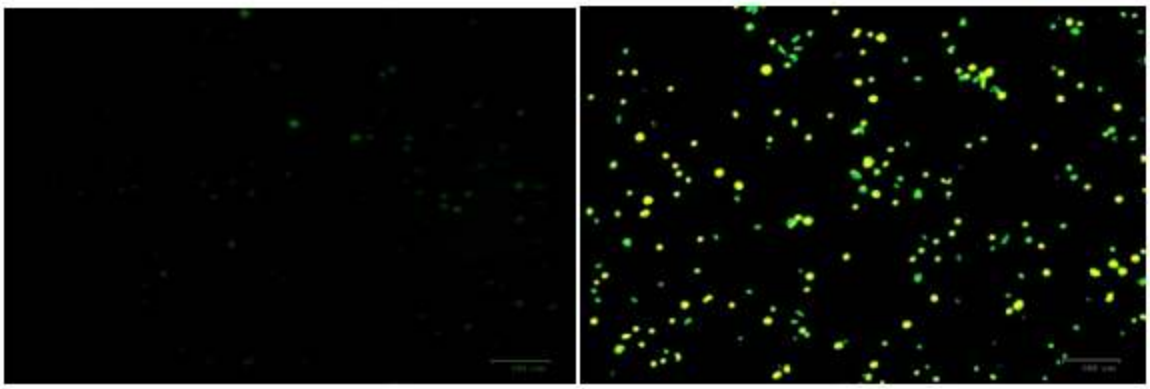

## Figure 4

GC-MS analysis of phycoerythrin




## Figure 5

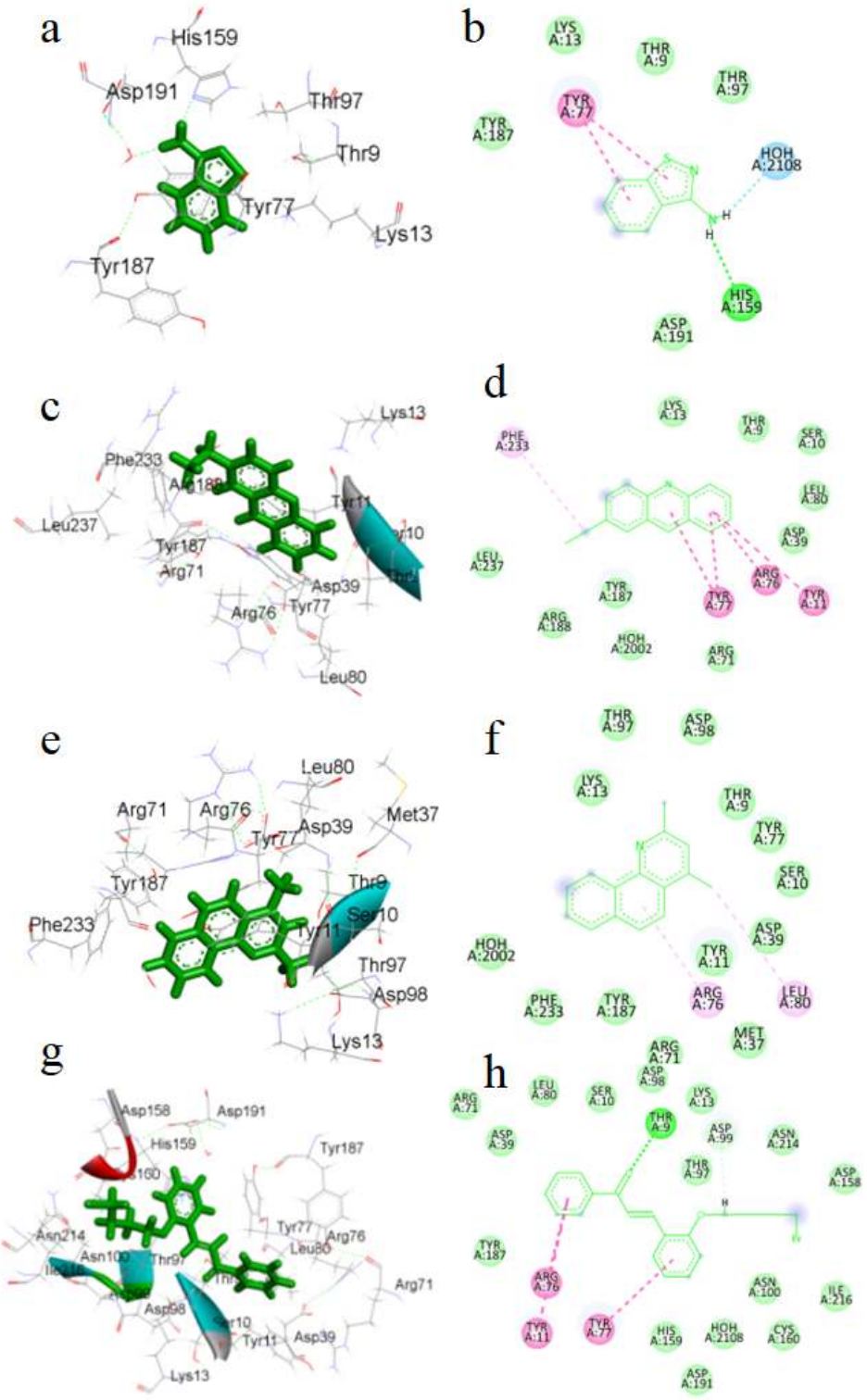
The morphological view of human lung cancer cells assesses the proliferation of cell inhibitory concentrations (50, 100, 200, 300, 400, and 500 µg $mL^{-1}$) of phycoerythrin pigment.



## Figure 6

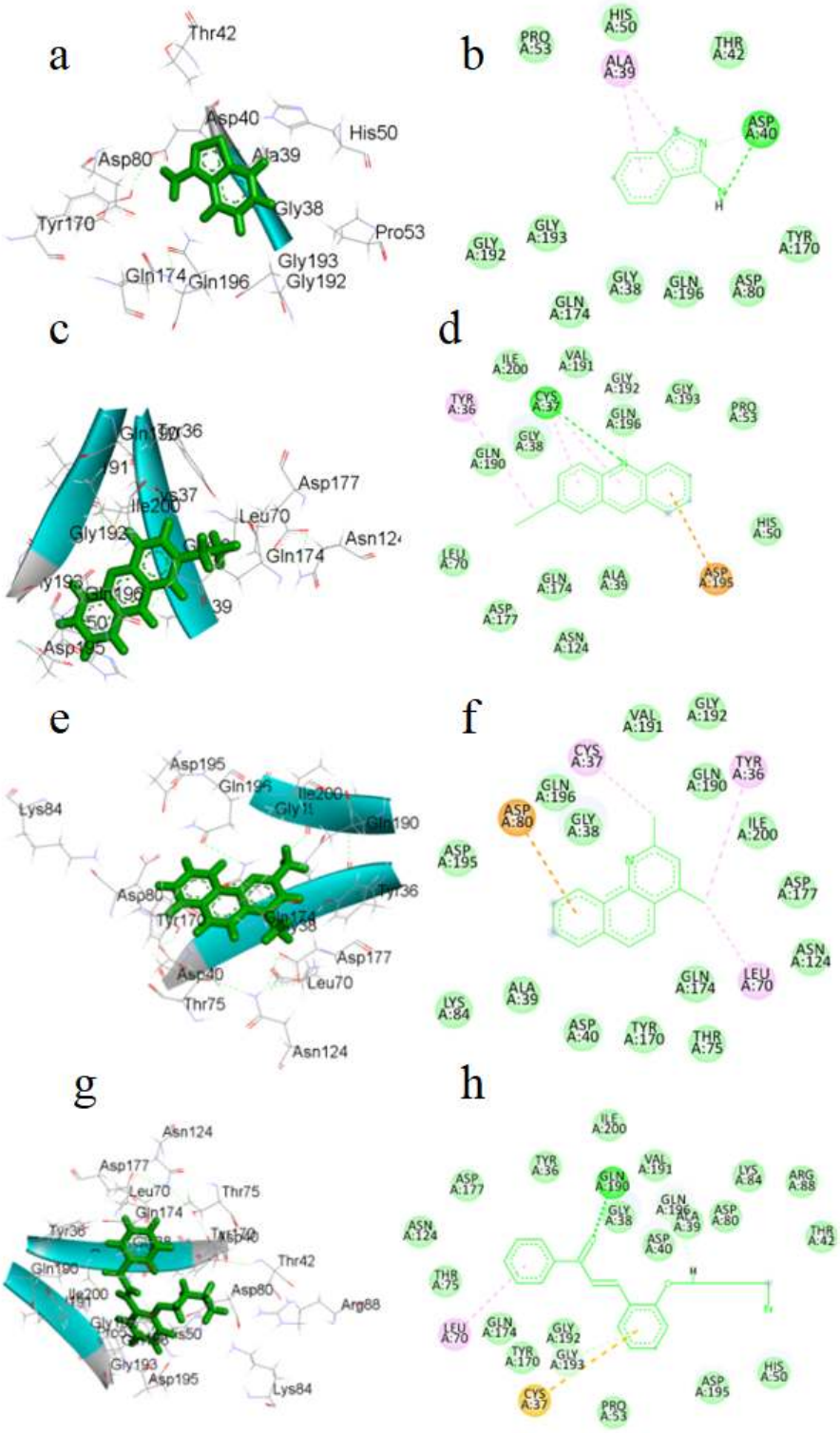
Phycoerythrin produces programmed cell death in human lung cancer cells. (a) Control cells exhibited a green color, signifying that the cells were alive; (b) Cells treated with phycoerythrin at a concentration of

203.4 µg mL⁻¹ displayed live cells (green color), dead cells (red color), and apoptotic cells (yellow color).



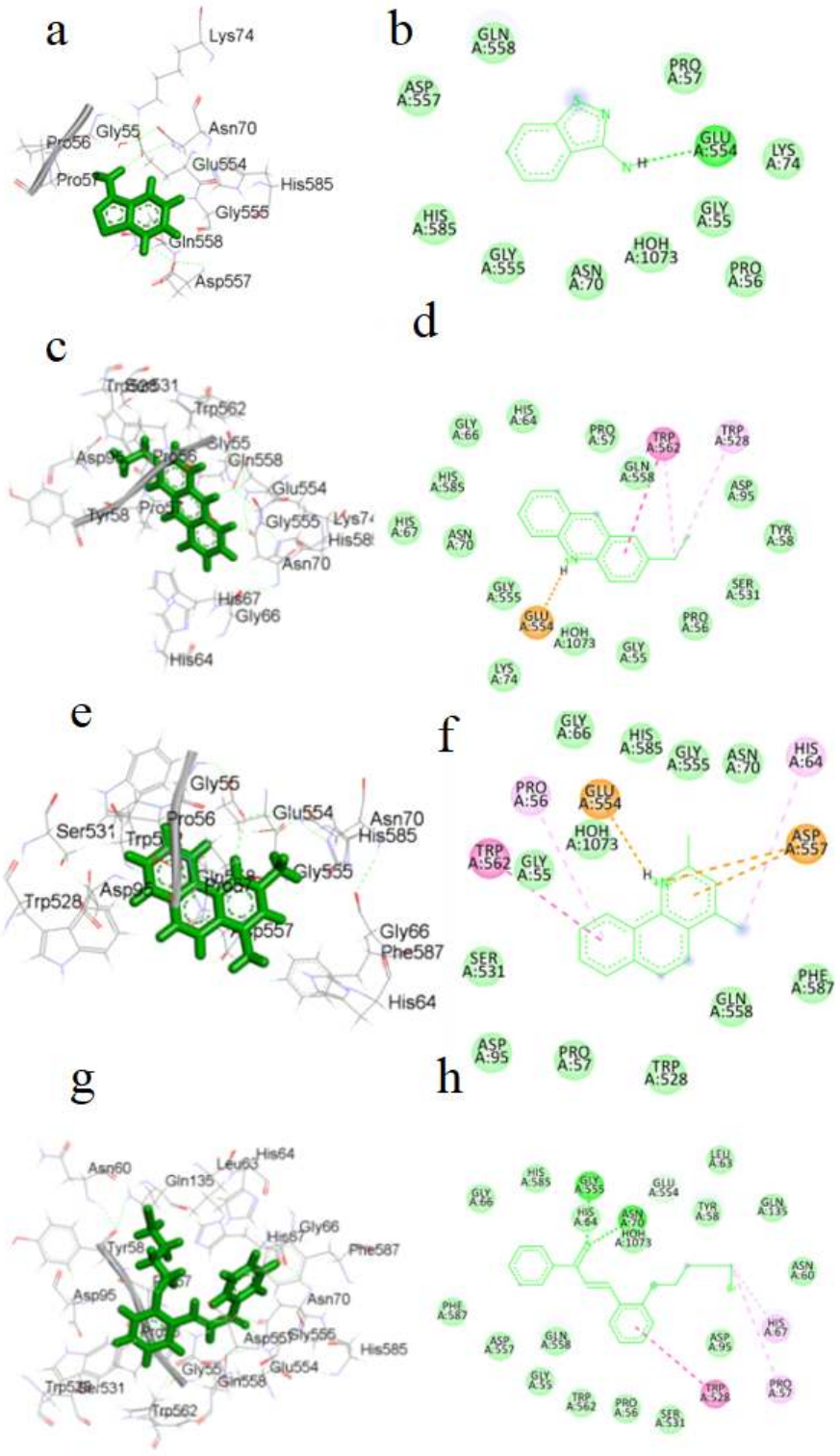

## Figure 7

The target protein Spore coat polysaccharide biosynthesis protein SpsA docked with the compound of three- and two-dimensional structure such as 1,2-Benzisothiazol-3-amine (a, b), 2-Ethylacridine (c, d), 2,4-Dimethylbenzo[h]quinolone (e, f), 2-bromobutyloxychalcone (g, h) respectively.



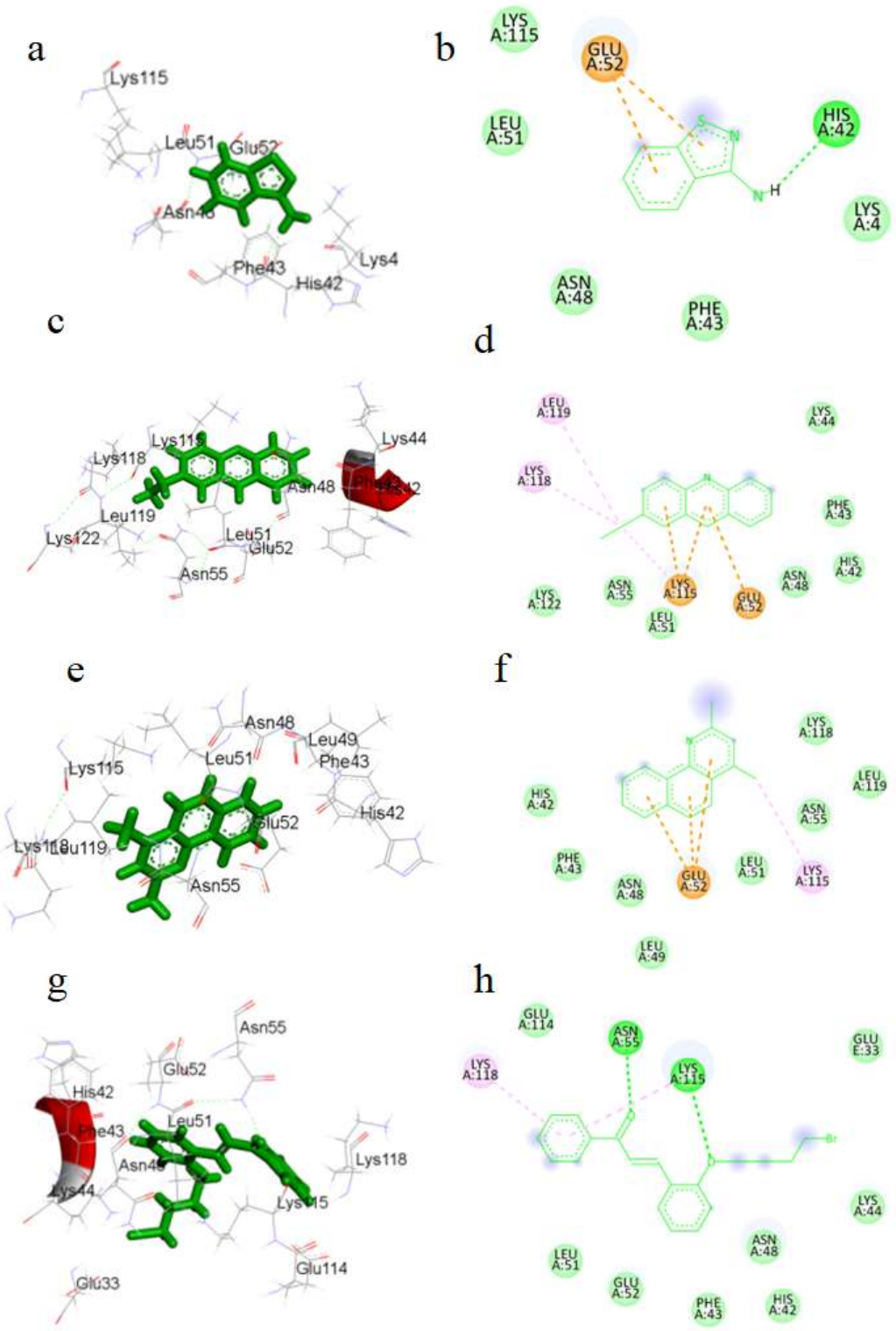

## Figure 8

The target protein *S. aureus* tyrosyl-tRNA synthetase docked with the compound of three- and two-dimensional structure such as 1,2-Benzisothiazol-3-amine (a, b), 2-Ethylacridine (c, d), 2,4-Dimethylbenzo[h]quinoline (e, f), 2-bromobutyloxychalcone (g, h) respectively.



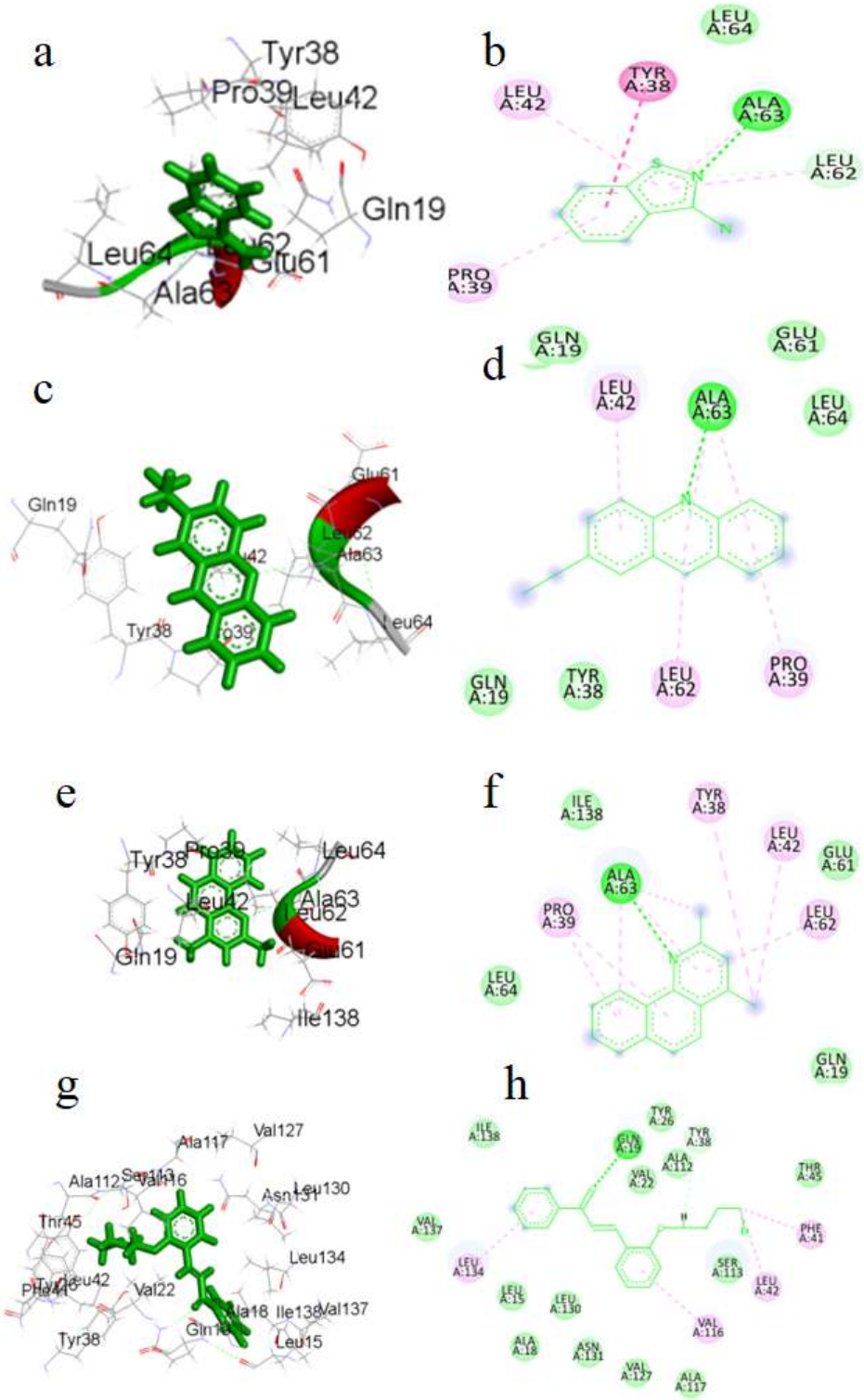

## Figure 9

The target protein Isoleucyl-tRNA synthetase docked with the compound of three- and two-dimensional structure such as 1,2-Benzisothiazol-3-amine (a, b), 2-Ethylacridine (c, d), 2,4-Dimethylbenzo[h]quinoline (e, f), 2-bromobutyloxychalcone (g, h) respectively.



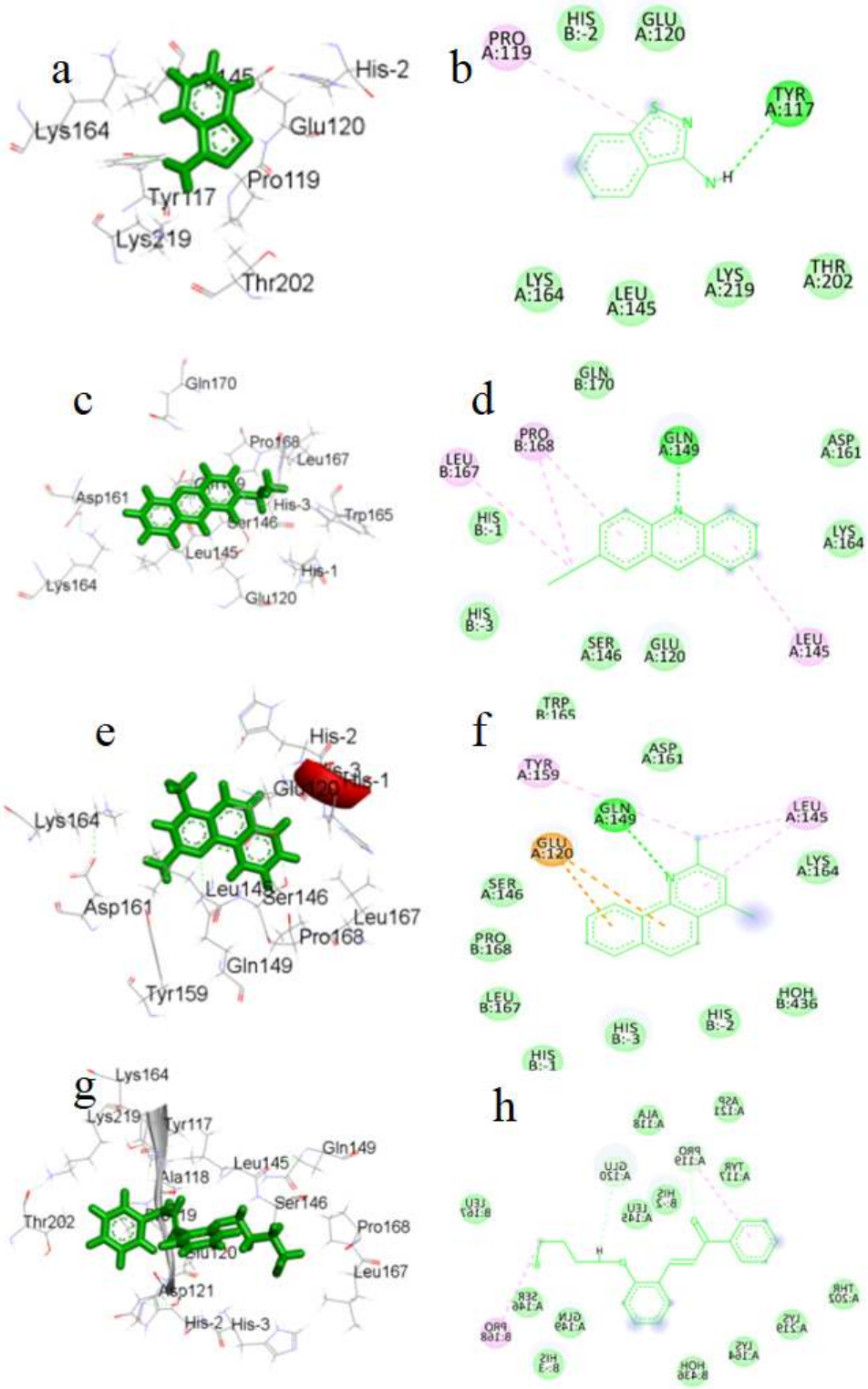

## Figure 10

The target protein Transcriptional regulator qacR docked with the compound of three- and two-dimensional structure such as 1,2-Benzisothiazol-3-amine (a, b), 2-Ethylacridine (c, d), 2,4-Dimethylbenzo[h]quinoline (e, f), 2-bromobutyloxychalcone (g, h) respectively.



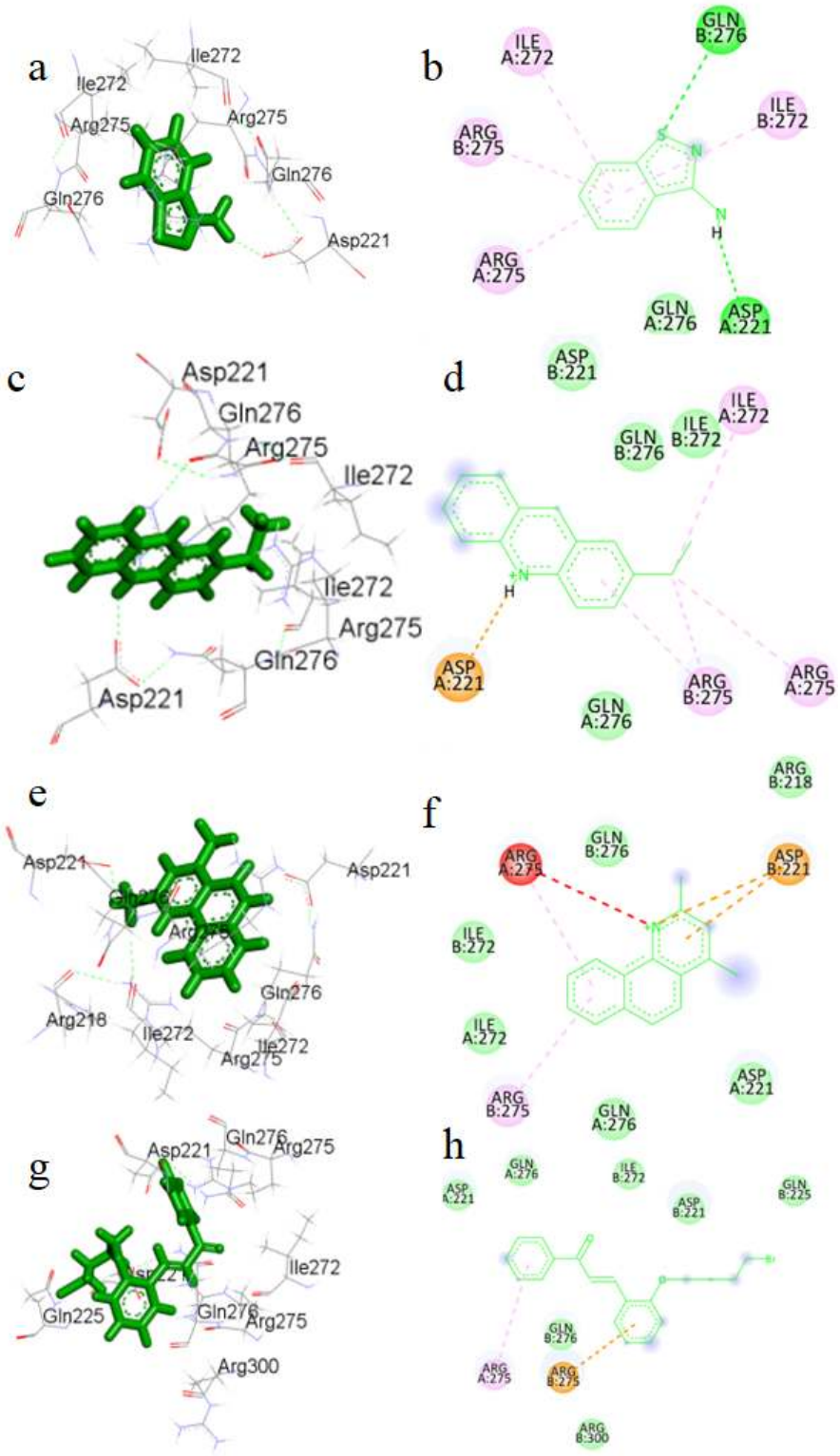

## Figure 11

The target protein HTH-Type Transcriptional Regulator MgrA docked with the compound of three- and two-dimensional structure such as 1,2-Benzisothiazol-3-amine (a, b), 2-Ethylacridine (c, d), 2,4-Dimethylbenzo[h]quinoline (e, f), 2-bromobutyloxychalcone (g, h) respectively.



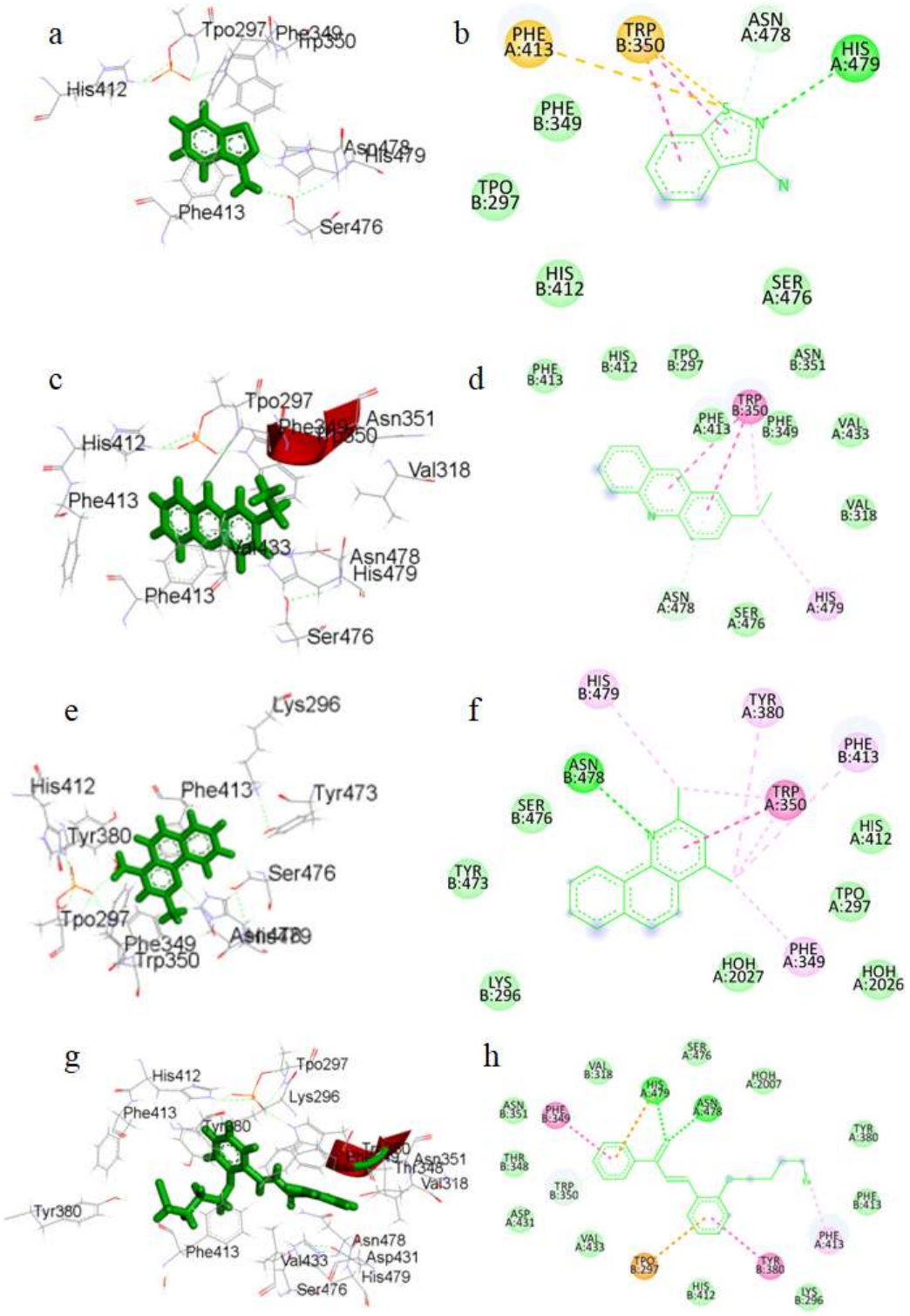

## Figure 12

YcgJ protein from *Bacillus subtilis* [PDB ID 2GLU] with the compound of three- and two-dimensional structure such as 1,2-Benzisothiazol-3-amine (a, b), 2-Ethylacridine (c, d), 2,4-Dimethylbenzo[h]quinoline (e, f), 2-bromobutyloxychalcone (g, h) respectively.



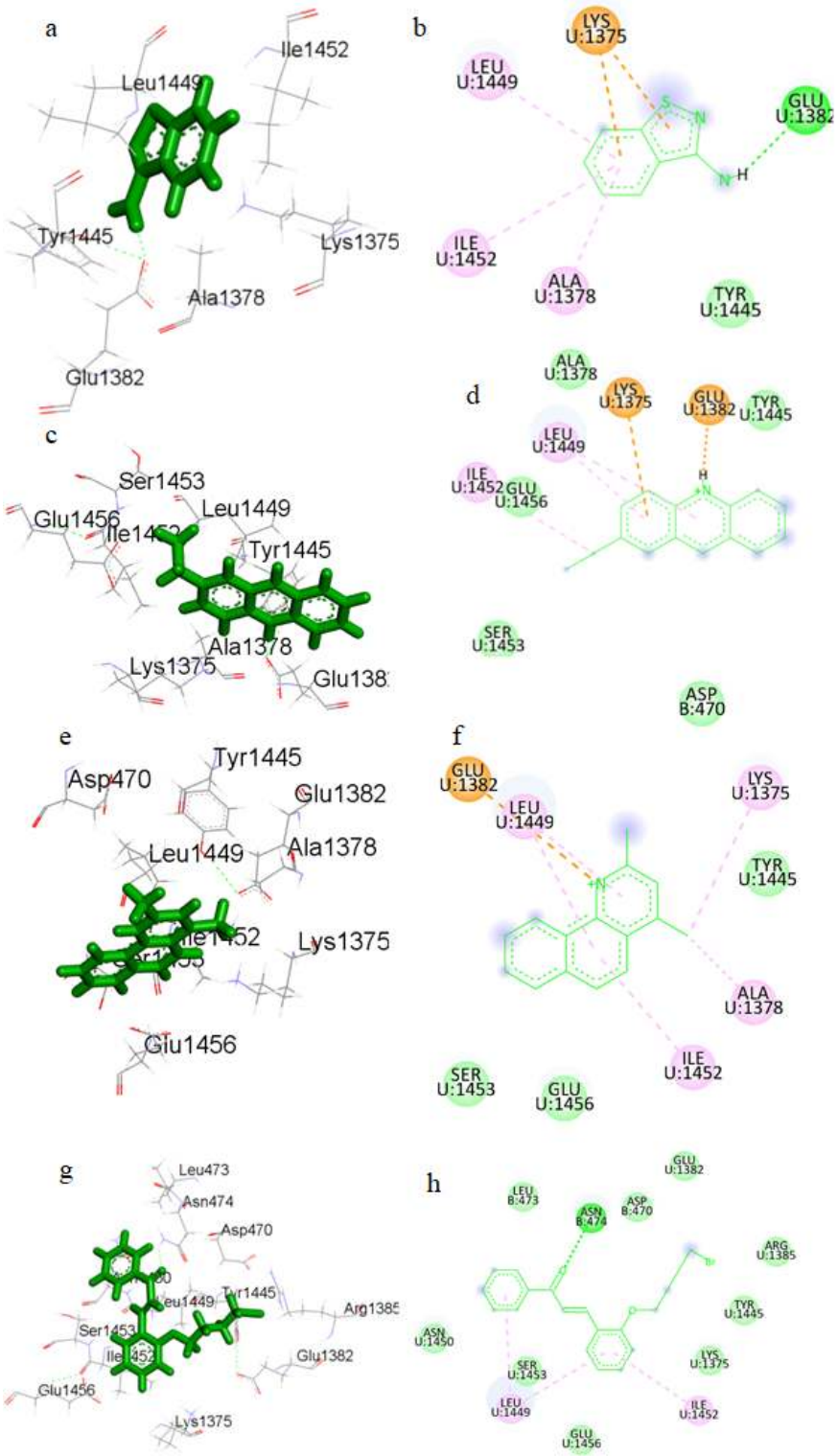

## Figure 13

The target protein Dihydropteroate synthase docked with the compound of three- and two-dimensional structure such as 1,2-Benzisothiazol-3-amine (a, b), 2-Ethylacridine (c, d), 2,4-Dimethylbenzo[h]quinoline (e, f), 2-bromobutyloxychalcone (g, h) respectively.



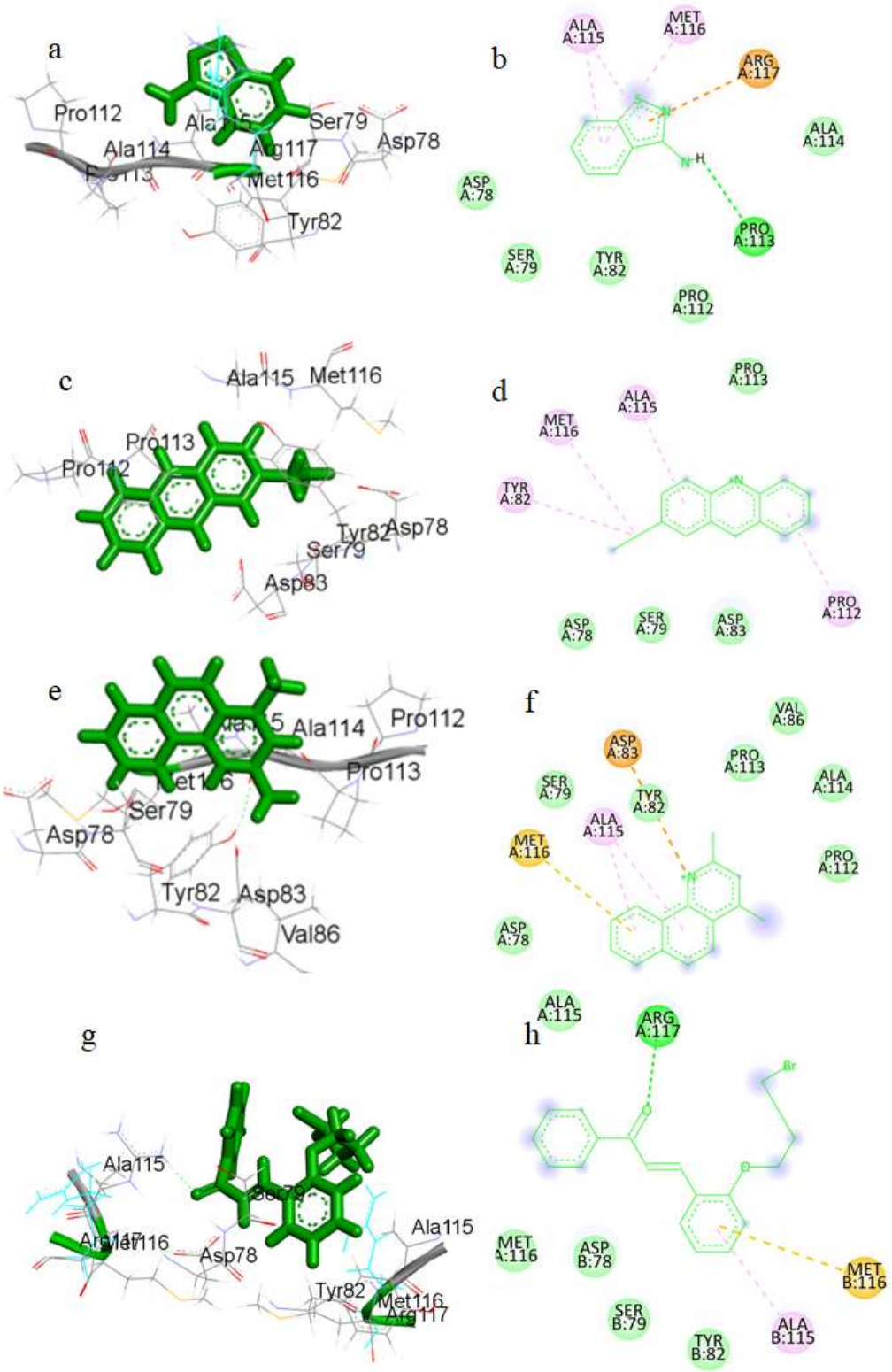

## Figure 14

The target protein Processed Glycerol Phosphate Lipoteichoic Acid Synthase 2 docked with the compound of three- and two-dimensional structure such as 1,2-Benzisothiazol-3-amine (a, b), 2-Ethylacridine (c, d), 2,4-Dimethylbenzo[h]quinoline (e, f), 2-bromobutyloxychalcone (g, h) respectively.



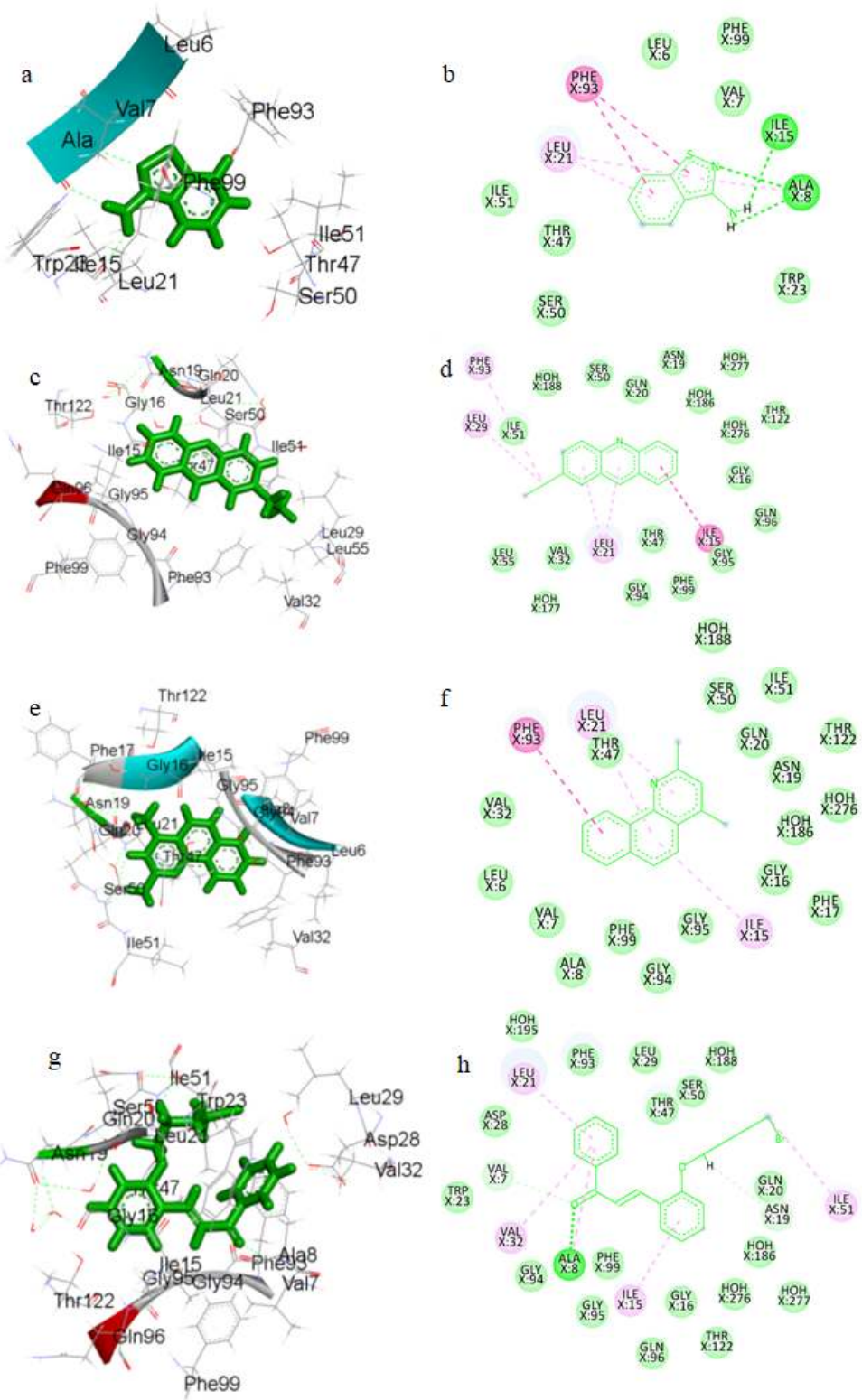

## Figure 15

The target protein DNA Gyrase Subunit B, DNA Gyrase Subunit A docked with the compound of three- and two-dimensional structure such as 1,2-Benzisothiazol-3-amine (a, b), 2-Ethylacridine (c, d), 2,4-Dimethylbenzo[h]quinoline (e, f), 2-bromobutyloxychalcone (g, h) respectively.



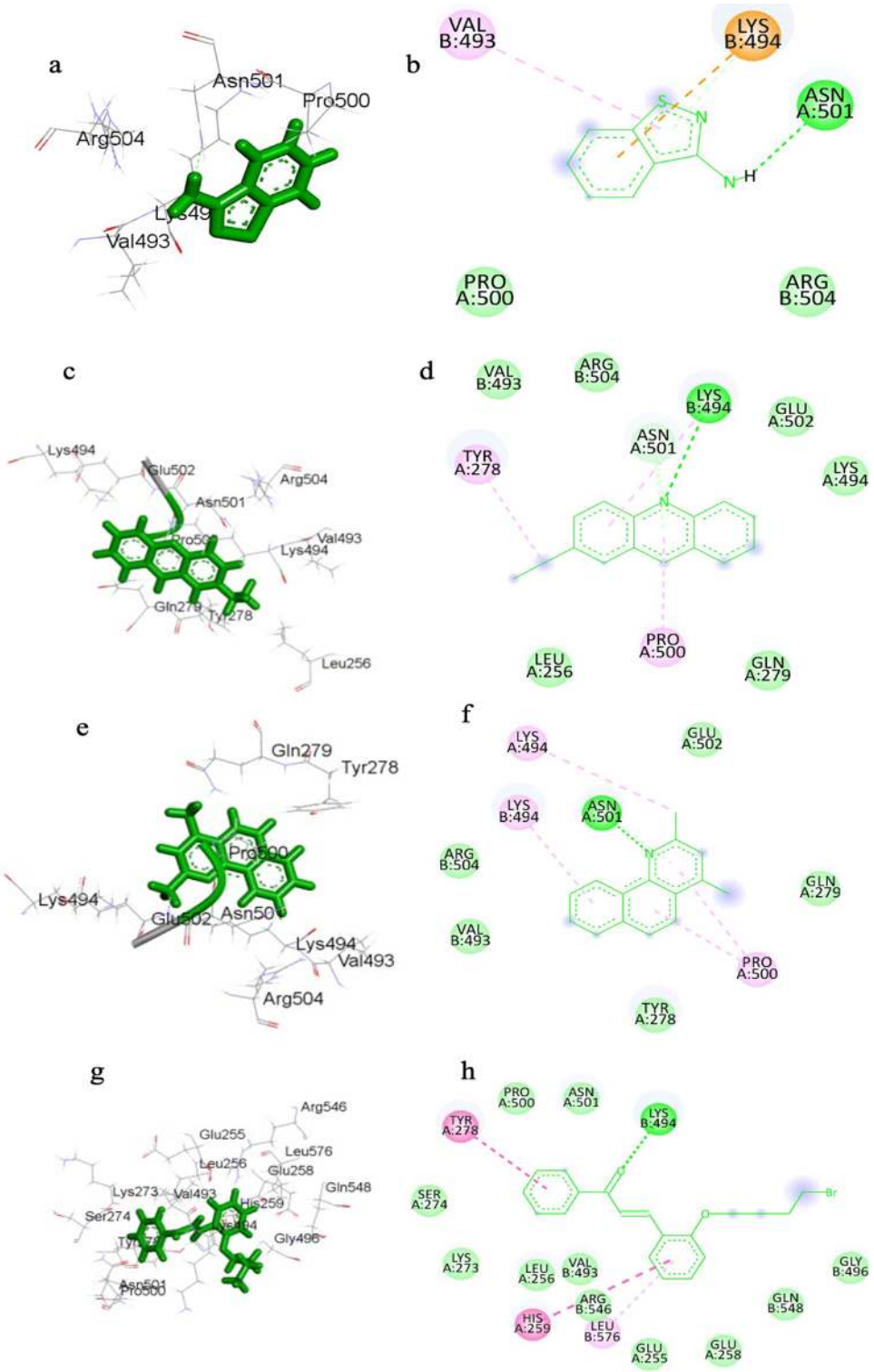

## Figure 16

The target protein DNA topoisomerase 4 subunit A docked with the compound of three- and two-dimensional structure such as 1,2-Benzisothiazol-3-amine (a, b), 2-Ethylacridine (c, d), 2,4-Dimethylbenzo[h]quinoline (e, f), 2-bromobutyloxychalcone (g, h) respectively.




## Figure 17

The target protein Dihydrofolate reductase docked with the compound of three- and two-dimensional structure such as 1,2-Benzisothiazol-3-amine (a, b), 2-Ethylacridine (c, d), 2,4-Dimethylbenzo[h]quinoline (e, f), 2-bromobutyloxychalcone (g, h) respectively.




## Figure 18

The target protein *Penicillin*-binding protein 3 docked with the compound of three- and two-dimensional structure such as 1,2-Benzisothiazol-3-amine (a, b), 2-Ethylacridine (c, d), 2,4-Dimethylbenzo[h]quinoline (e, f), 2-bromobutyloxychalcone (g, h) respectively.

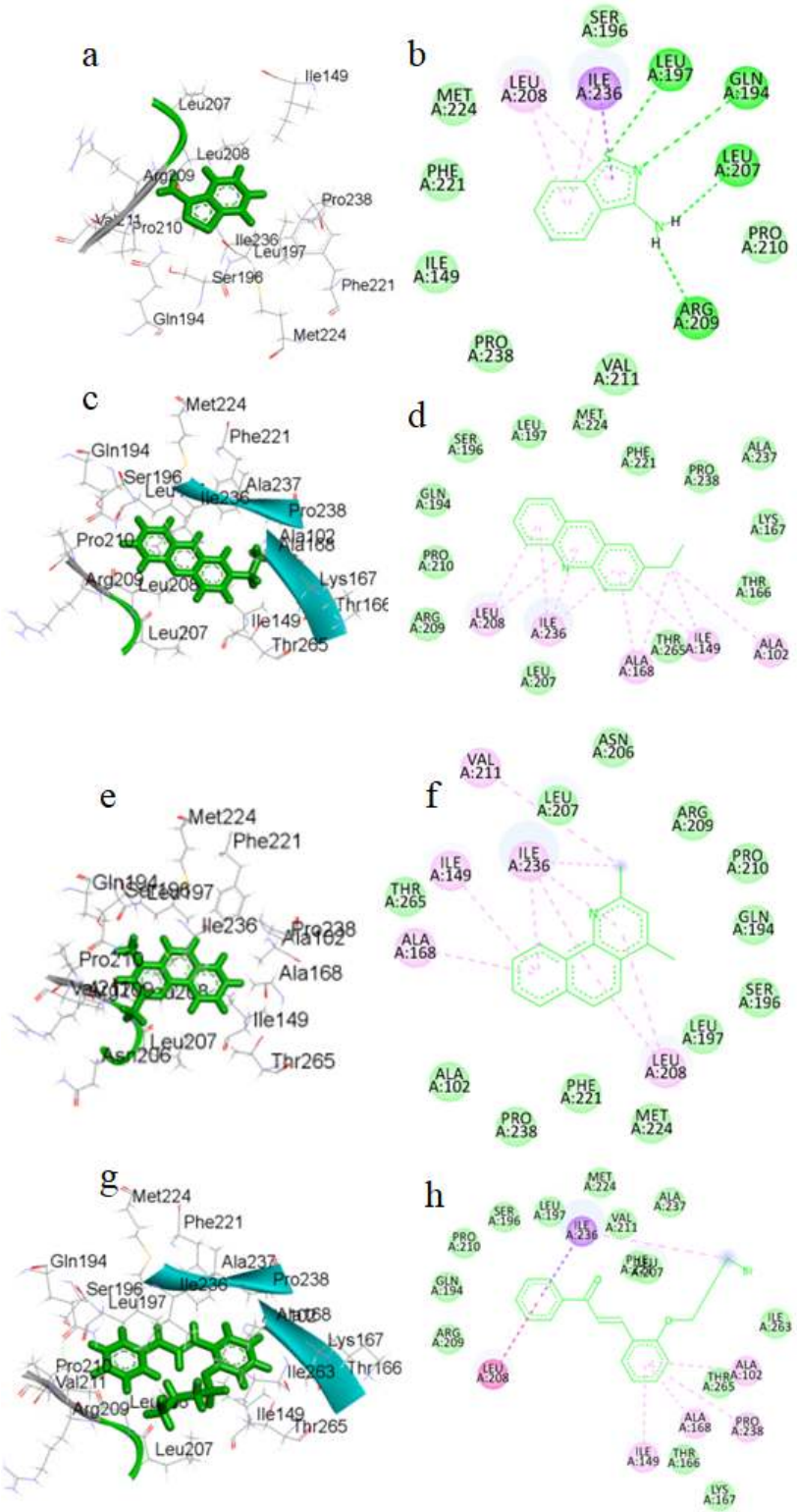



**Figure 19**

The target protein Transcriptional regulator MvfR docked with the compound of three- and two-dimensional structure such as 1,2-Benzisothiazol-3-amine (a, b), 2-Ethylacridine (c, d), 2,4-Dimethylbenzo[h]quinoline (e, f), 2-bromobutyloxychalcone (g, h) respectively.

# Supplementary Files

This is a list of supplementary files associated with this preprint. Click to download.

- Annexure.docx